Impact of climate variability on wind and solar energy production, on heating consumption and on atmospheric dispersion of pollutants

Larsen, Søren Ejling; Kristensen, Leif; Frydendahl, K.

Publication date:
1988

Document Version
Publisher's PDF, also known as Version of record

Risø-R-558

Impact of climate variability on wind and solar energy production, on heating consumption and on atmospheric dispersion of pollutants

S.E. Larsen, L. Kristensen and K. Frydendahl

Abstract. The variability in the potential for wind and solar energy production over the last 100 years is inferred from series of Danish meteorological measurements established in the period 1873–1982. From the same data series is estimated also variability in the use of energy for heating of houses and the ability of atmosphere to disperse air pollution.

March 1988

Risø National Laboratory, DK-4000 Roskilde, Denmark

The report is a summary of results obtained and work made under Contract No. CLI-049-DK between CEC, DGXII and Risø within the First R&D Programme in the field of climatology.

ISBN 87-550-1407-0
ISSN 0106-2840

Grafisk Service, Risø, 1988

Contents

1 Introduction

The purpose of the project summarized here has been to evaluate the variability in climate parameters of importance to energy and environmental questions in Northwestern Europe.

Whenever weather data are important for evaluating these kinds of questions, one usually satisfies oneself with data from the last 5-20 years, because this is the period giving the most readily available high-quality data. However, many solutions to energy and environmental problems of today have a lifetime exceeding 20 years. Larger industrial production of processing units (including power plants) will often have a lifetime of 20-30 years while systems of the infrastructure type (electric power and natural gas lines) will have an even longer life. Many environemtal problems can be considered as short-term problems whereas others are associated with long-term processes. As an example of the latter we mention aspects of the problems associated with deforestation and pollution of the European coastal waters.

Therefore, a study of the kind of variability to be found in our recent climate history seems reasonable both to describe our current status and because the variability encountered in the recent past can be taken as null hypothesis for the variability to be encountered in the near future.

2 Data selection and organisation

The study of recent climate variations in Denmark is most logically based on the meteorological records compiled by the Danish Meteorological Institute. These records comprise more than 20 stations started in the beginning of the 1870'es. Some of the data have been transferred to magnetic tapes, but owing to lack of resources at the Meteorological Institute the digitised data have been screened and organised for further analysis only to a small extent.

At the onset of this project the work with the data series presented itself as a major problem of quite unknown complexity.

We therefore decided to start with the data series obtained from the climatic station at Fanø. Hereby we hoped to familiarize ourselves with the data problems associated with the data series in question. Fanø was chosen for two reasons; first, it is placed at the southwestern coast of Denmark, see Fig.2.1. With the southwesterly winds dominating in Denmark the Fanø climatic station can therefore be said to record a kind of upstream conditions of the country. Secondly and even more important, it was the only series that was systematically screened for some of the observed parameters (Brown et al., 1983).

Simultaneously with the analysis of the Fanø data the current climate of Denmark was surveyed on the basis of available literature and compiled data (Larsen and Jensen, 1983). The purpose of this study was partly to establish a framework of current climate within which to understand the temporal variability emerging from the analysis of the Fanø data and on the basis of which to choose the next long data series to be included in the analysis.

From Larsen and Jensen (1983) we can summarize the Danish climate: the country has a maritime temperate climate dominated by westerly winds and frequent passings of low- and high-pressure systems. As a result, the "usual" Danish weather is dominated by cool and unsteady summers and warm and changeable winters. However, it happens occasionally that easterly winds dominate, carrying to the country the severe winters and hot summers of the continent. In terms of geographical variation this means

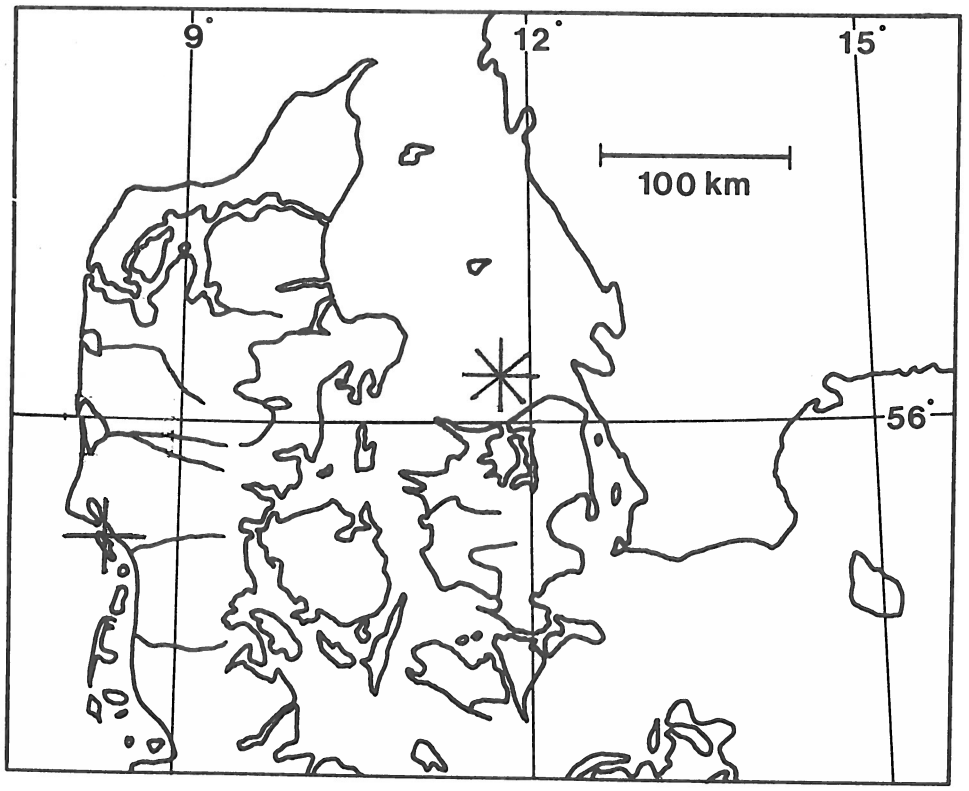

Figure 2.1. Map showing the position of the Fanø(+) and Hesselø (*) climatological stations.

that the Danish climate becomes more continental on two scales: moving inland where the diurnal variation becomes more pronounced, and moving east where one comes closer to the continent and the seasonal variation becomes more pronounced. Since the frequency of the above-mentioned period with easterly winds is of great importance to the variability of the Danish climate, we expect this variability to be more pronounced in the eastern part of Denmark. The current climate of Denmark is summarized in Table 2.1.

Table 2.1. Short summary of the Danish climate. The table displays yearly average, seasonal and typical variations across the country of monthly averages of key climatic parametres (Larsen and Jensen, 1983).

Parameter	Monthly averages				Units
	Yearly average	Yearly variation		Geographical variation	
		Minimum	Maximum		
Temperature	8	-0.5	16.6	1	°C
Hours with sunshine	144	30	290	10% of value	hr/month
Relative humidity	82	72	91	10	
Cloud cover	64	53	78	20	% of sky
Precipitation	55	34	81	20	mm/month
Wind speed 10 m above terrain	5	4	6.5	2	m/s

The climatic variability depicted by the Fanø data is extensively reported in Peterson (1983), Peterson and Larsen (1983, 1984a), Larsen (1985) and Nielsen and Hansen (1986). The emerged picture is in accordance with the description given by Lamb (1969) of the Northwestern Europe with a more continental type of climate in this century than before. The trends depicted by the Fanø series are summarized in Fig. 2.2.

In general, the analysis of the Fanø series showed a fairly reliable appearance of the series in the sense that it depicted the same climatic variability as was found for the region as a whole. Also the behaviour of the different parameters was found to support each other. The main difficulty of the Fanø series was associated with the wind speed observations. For several reasons these were difficult to analyse, including

Table 2.2. Brief summary of the observations at Fanø and Hesselø.

Station	Hour of obs.	Parameter	Year
Fanø	0800 1400 2100	wind speed, direction, cloud cover, temperature, pressure, humidity	1873-1982
	0800	daily precipitation, max/min temperature	
Hesselø	0400, 0800 1400, 2000 2400	wind speed, direction, cloud cover*	1873-1970
	0800 1400 2100	wind speed, direction, cloud cover	1971-1982
		temperature	1873-1982
		pressure, humidity	1960-1982
	0800	max/min temperature	1873-1982
		daily precipitation	1960-1982

* Until 1908 the cloud cover values were obtained by converting the observed parameter called "type of weather"to cloud cover.

1. wind speed and directions had been estimated subjectively rather than objectively measured by instruments
2. observers and to some extent sites changed over time
3. the scale in which the wind was reported was changed from a 7-category land scale before 1911 to a 13-category Beaufort scale in the years after 1911.
4. Roughness surroundings have changed over time, compare Fig. 2.3.

By comparing different segments of the series it was possible to find a relation between winds observed in the 7- and the 13-category scale, which were consistent with the data (Peterson, 1983, Peterson and Larsen, 1984b). However, the associated analyses clearly showed the need of better wind data.

In accordance with the above this need was given highest priority when choosing the next station for a climate data analysis. The station chosen was placed in connection with a lighthouse on the small island of Hesselø in the Kattegat, see Fig. 2.1. From a wind observation point of view the lighthouse stations in Denmark have the advantage that they were manned around the clock by teams taking turns. This meant that observations of wind and cloud cover were performed both day and night, compare Table 2.2. Also, it ensured a better continuity in the perception of the wind speed scale by the members of the teams. Last but not least the wind observations of the lighthouse were made in the Beaufort scale since the start of the observations in 1873, and the surrounding surface roughness has been that of water during the entire duration of the data series. compare Fig. 2.3. The drawback of the lighthouse observations is that they generally include less parameters.

In connection with the discussion in the beginning of this section about geographical variations of the Danish climate it is seen that by choosing Hesselø we obtained an easterly station very much reflecting the conditions over the Kattegat. Accordingly, we will expect the Hesselø station to show less diurnal variation but a somewhat larger seasonal and climatic variability. In the following section we shall use bolth Fanø and Hesselø data whenever reasonable.

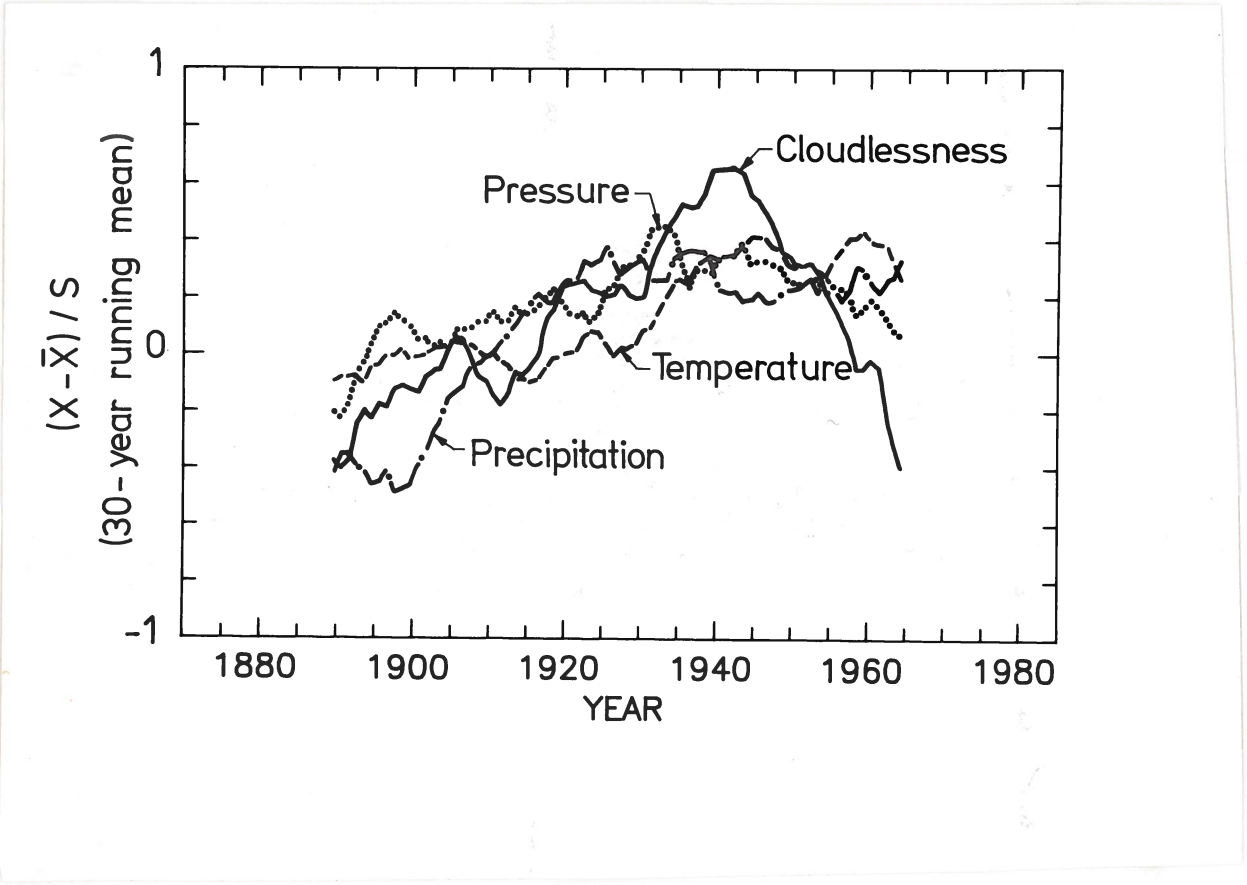

Figure 2.2. Normalized 30-year running means of pressure, temperature, precipitation and cloudlessness from Fanø. Variables are normalized by their respective mean and standard deviations. $\bar{x}$ is the mean of the variable of the total record (1875-1980) and S is the standard deviation of the yearly average of the variable. Cloudlessness is defined as the negative cloud cover (Peterson and Larsen, 1984a).

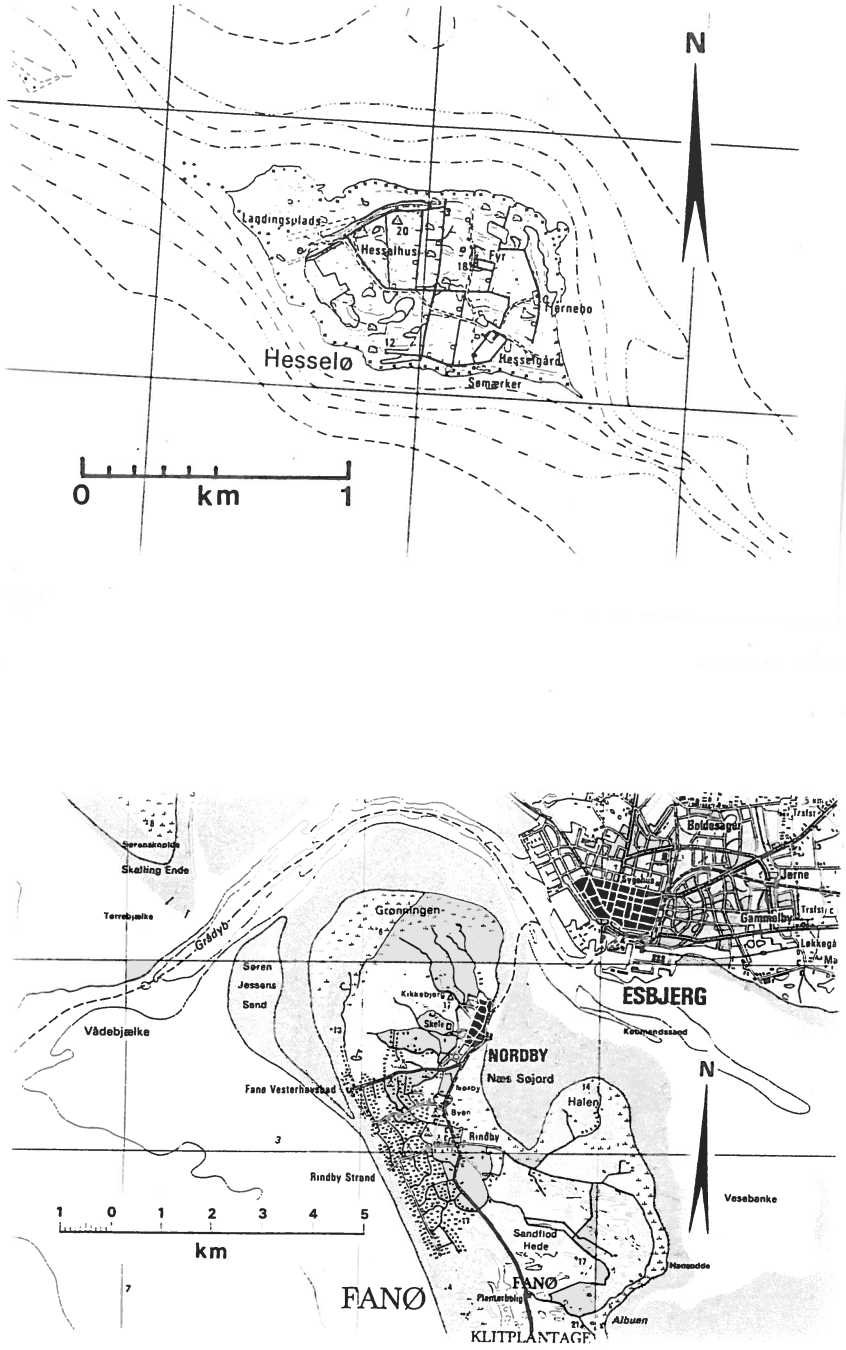

Figure 2.3. Detailed maps of the surroundings of the climatological stations at Fanø and Hesselø. During its history the Fanø station has been moved around within the Nordby area. The Hesselø station has been at the lighthouse (fyr) with the exception that the temperature measurements were performed at Hesselgaard in the period 1963-82.

3 Results on energy and dispersion

In this section we shall address the main questions of this project on the basis of the Fanø and Hesselø data. The questions concern the climatic variability of

1. energy consumption for heating purposes
2. solar energy potential
3. wind energy potential
4. atmospheric dispersion

Mainly we will present our results in terms of time series of consecutive 5-year mean values. The choice of five years as our basic average is somewhat arbitrary. A reason is, however, that a period of 5-10 years tends to be the usual length of meteorological records used for evaluating energy or environmental questions.

3.1 Climatic variation in energy needed for heating purposes

A generally used parameter for estimating energy needs for heating purposes in a certain period is the so-called heating degree days. The number of heating degree days per day is defined as

$$HDD = \begin{cases} T_B - T & \text{for} T \leq T_B \\ 0 & \text{for} T \geq T_B \end{cases} \quad (1)$$

Here T is the daily mean temperature. For a number of reasons it is recommended to compute T from the daily maximum and minimum temperatures as follows

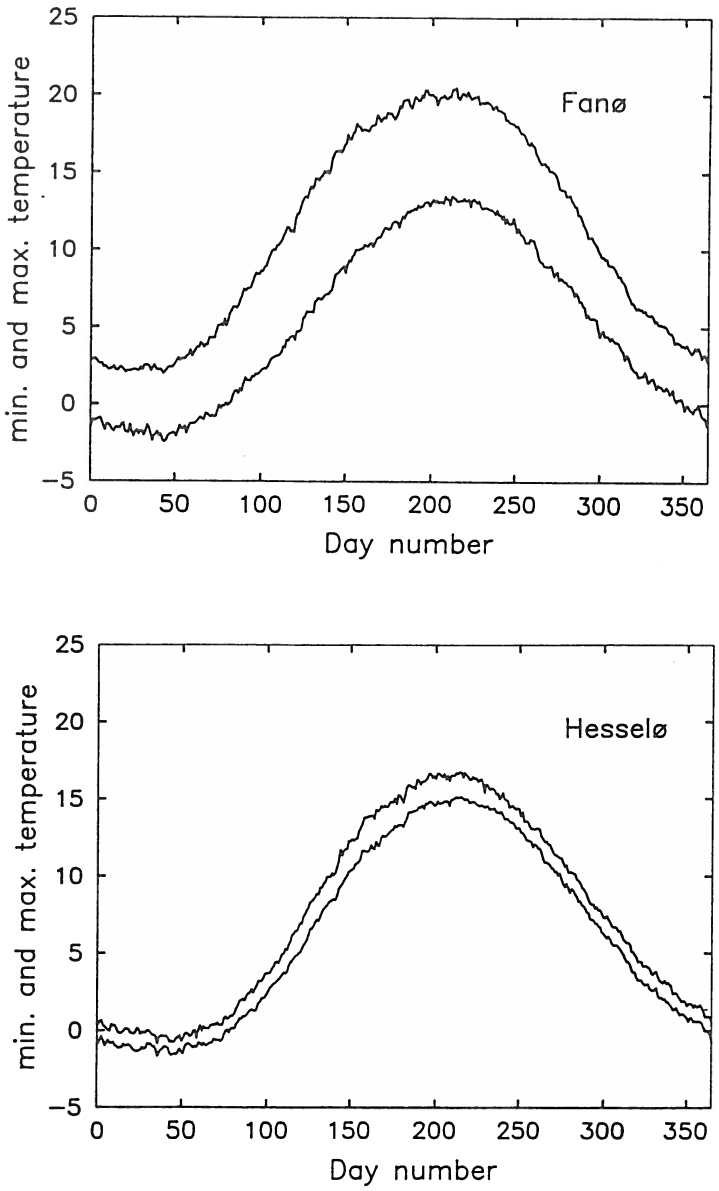

Fig. 3.1. The annual variation of the daily maximum and minum temperatures at Fanø and Hesselø averaged over the total record.

$$T = \frac{1}{2}(T_{max} + T_{min}).$$

T_B is a basic temperature that usually varies from country to country. In Denmark is used $T_B = 17°C$, which is the value employed here.

The energy, E, needed for heating during a period of, say n days is proportional to the total number of heating degree days for the said period

$$E = k \cdot \sum_{i=1}^{n} HDD_i. \tag{2}$$

Occasionally an attempt is seen to modify the empirical factor k with functions including wind speed and in- and outgoing radiation at the surface. However, these efforts often result in little improvement of the accuracy of Eq. (2) or impprovement is obtained, but the equation becomes of more specialized validity for specific types of houses in specific surroundings, etc. Therefore, we shall use only the number of heating degree days in consecutive 5-year periods to evaluate the variation of energy needs. First, we illustrate the behaviour of the temperature records at the two stations.

Figure 3.1 shows the annual variation of the maximum and minimum temperatures averaged over the whole period of observation. As discussed in section 2 Hesselø is clearly seen to be more maritime than Fanø as the difference between daily maximum and minimum temperatures is much smaller at Hesselø. Less clearly seen is that Hesselø has a slightly larger annual amplitude ($\sim 1.5°C$) in keeping with its more easterly location, which makes it more continental on the seasonal time scale, see section 2.

Figure 3.2 shows the variation of consecutive 5-year average temperatures for the two stations. The larger climate variability at Hesselø is obvious. The deviations between the two records in the beginning of this century are large enough to rise suspicion about data errors. However, a closer study of the data records and measurement procedure has revealed no data errors large enough to explain the differences shown in the figure.

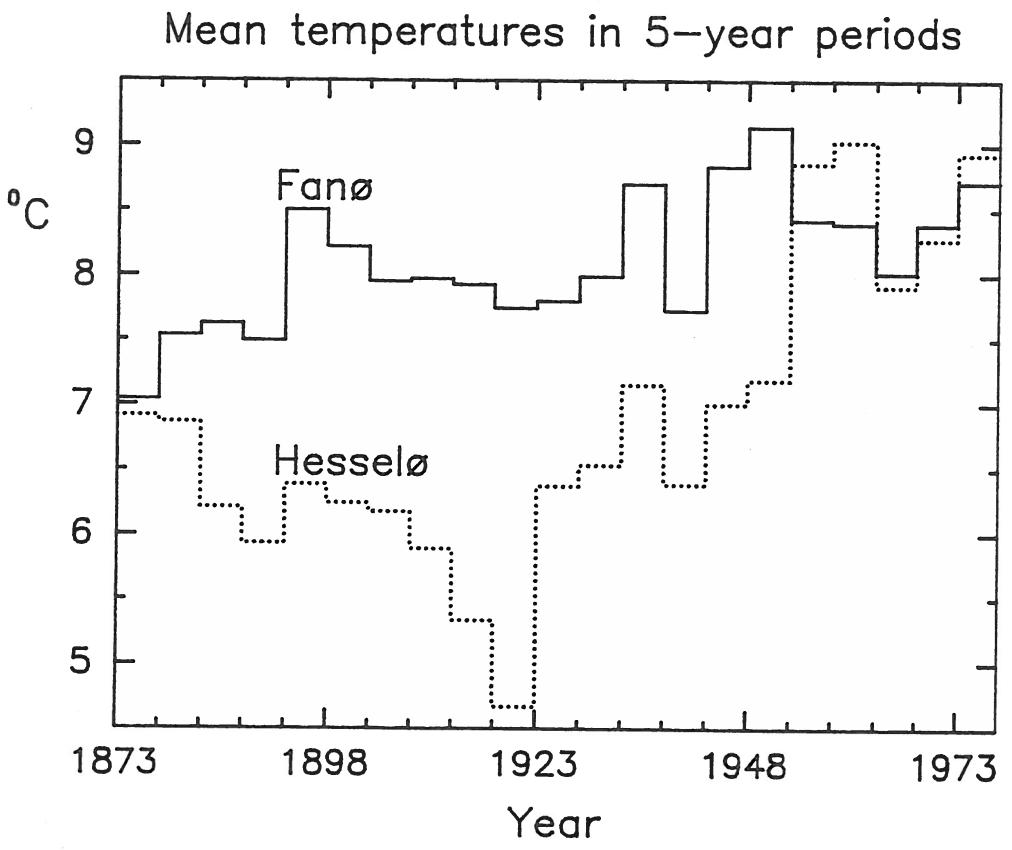

Fig. 3.2. Five-year mean values of temperature at Fanø and Hesselø.

Notwithstanding the differences the two data series agree with each other that Denmark has experienced an increase in the average temperature since the 1870es. The behaviour of the temperature series of course shows up also in the number of heating degree days for each 5-year period as shown in Fig. 3.3. The curves indicate a long time reduction of about 10 per cent in the heating degree days since the start of these measurements. Through Eq. (2) this translates to a 10 per cent reduction in the heating bill if all other factors were constant. The curves also indicate a maximum variation in the number of heating degree days of 10-20 per cent from one 5-year period to the next, which again translates to a corresponding variability in the heating expenses.

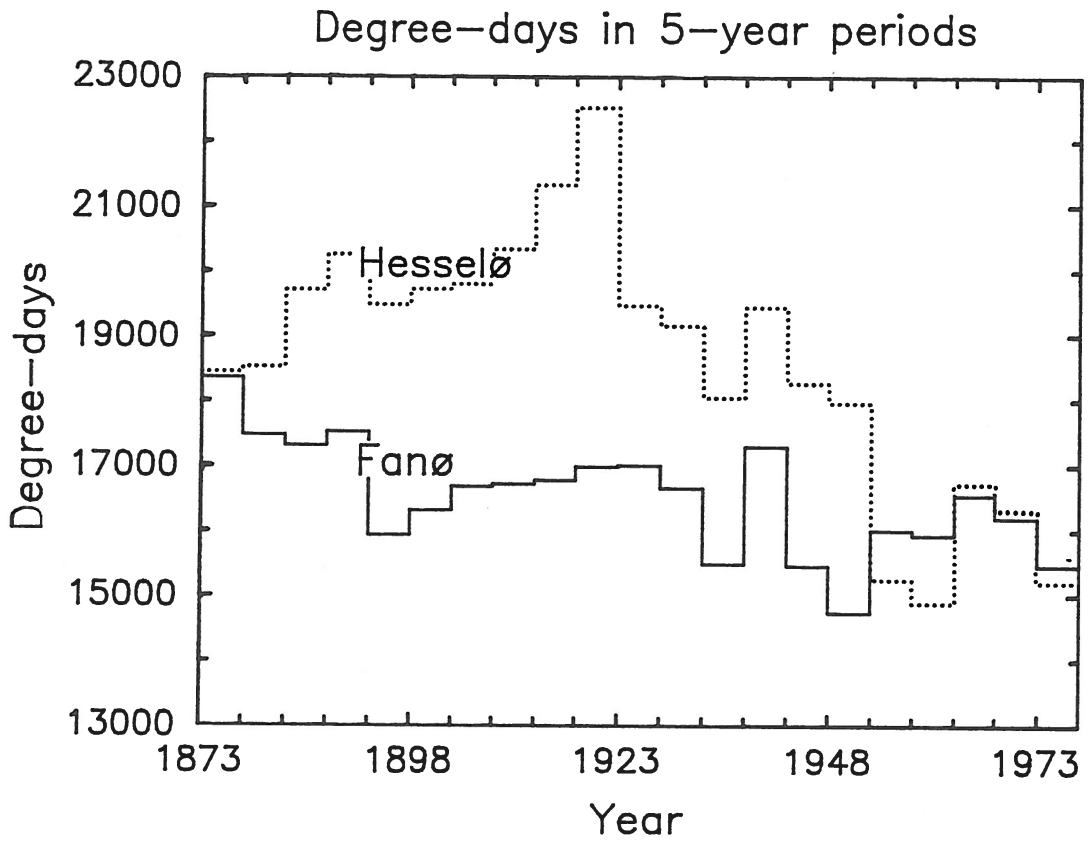

Fig. 3.3. Number of heating degree days in consecutive 5-year periods at Fanø and Hesselø.

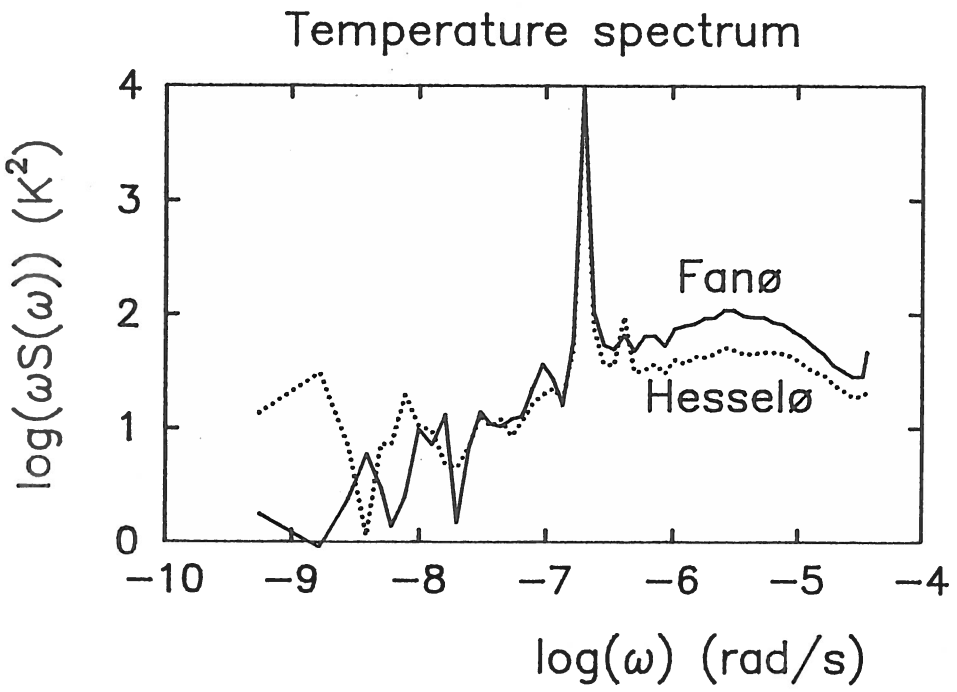

Fig. 3.4. Power spectrum of the daily mean temperature. The yearly period corresponds to about $2{\cdot}10^{-7} rad/s$.

As the degree days are so closely related to temperature we shall finish this section by illustrating the variability of temperature at Hesselø and Fanø in the terms of power spectra of temperature as shown in Fig. 3.4. Relative to the Fanø spectrum the Hesselø spectrum is seen to reflect somewhat less energy in time scales less than a year and somwehat more energy in the longest time scales.

3.2 Variation in available solar energy

If we assume the solar constant to be unchanged for the period the surface will mostly be controlled by variation in cloud clover.

Here the following procedure was used. The position of the sun in the sky was determined as a function of station latitude and longitude and on local time by a procedure described in Blackadar (1984). The accuracy is that of the almanac over a period of 10,000 years. With the solar altitude, φ, known at the times of observation, the incoming solar radiation was determined by a relation suggested by Holtslag and Van Ulden (1983) on the basis of measurements by the Dutch Meteorological Institute at De Bilt and Cabauw. The relation is of the type

$$K^+ = (a_1 \sin\varphi + a_2)(1 + b_1(N/10)^{b_2}) \qquad (3)$$

where K^+ is the incoming radiation and N is the cloud cover (0-10). a_1, a_2, b_1 and b_2 are empirical constants with $a_1 = 990$ and $a_2 = -30w/m^2$, respectively, b_1 = -0.75 and b_2 = 3.4. The accuracy of Eq. (3) is not impressive. Holtslag and Van Ulden found the standard deviation to increase with increasing values of N, and it can be as large as 40 per cent. Since the microclimate at Fanø is quite similar to that at the Dutch sites from where the constants in Eq. (3) were obtained, we expect that this equations will work quite well at Fanø. As far as the Hesselø data are concerned the maritime nature of the Hesselø station adds a component of uncertainty. However, more accurate formulas demand a more detailed knowledge of the type of cloud cover, and since this is not available in the data, we decided to use Eq. (3) being one of the more recent results from a climate almost like that of Denmark.

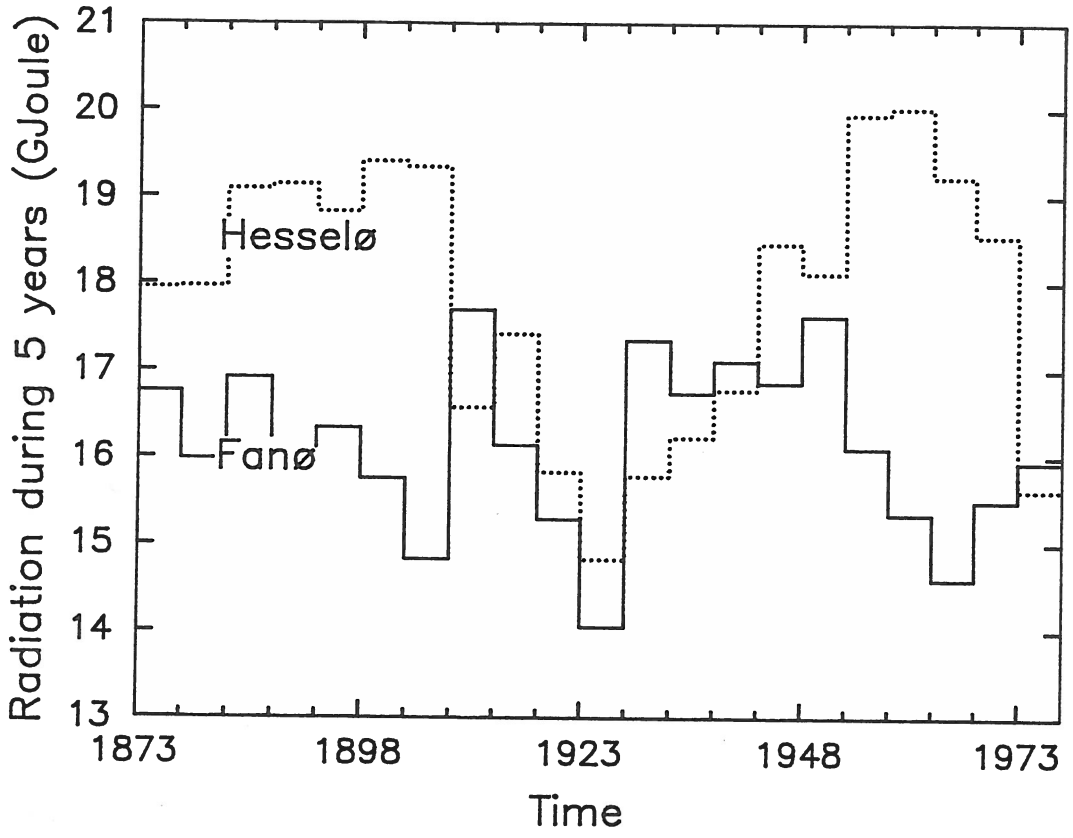

Fig. 3.5. Accumulated solar energy received at Fanø and Hesselø in consecutive 5-year periods. The values are estimated from the cloud cover.

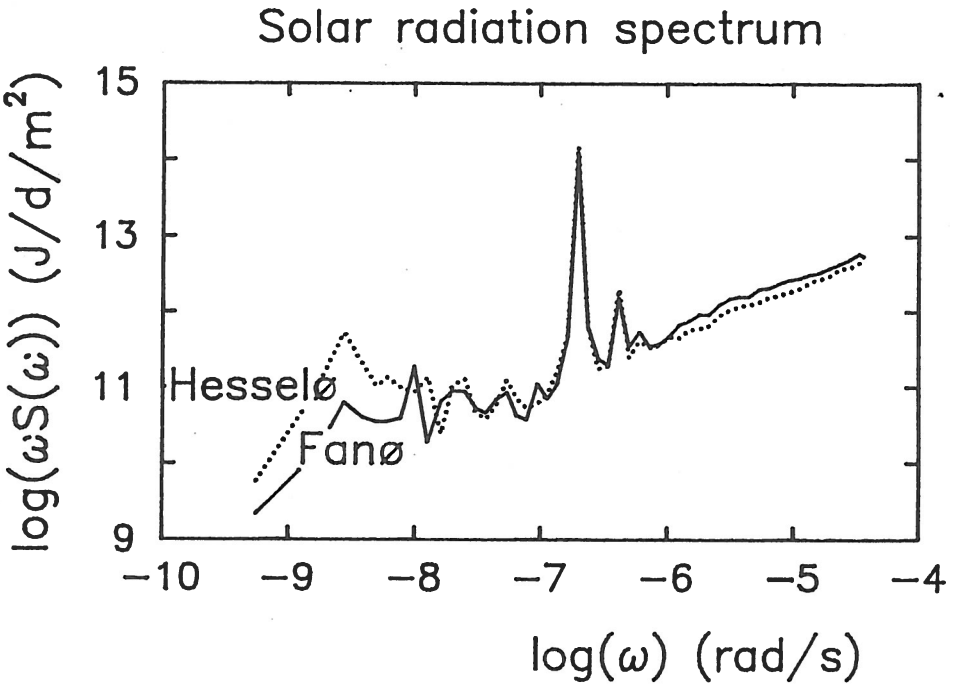

Fig. 3.6. Power spectrum of the daily solar radiation as computed from the cloud cover at Hesselø and Fanø.

With the incoming solar radiation determined at the times of observation the daily total was integrated by connecting the observed values by straight lines including the two zero points at sunrise and sunset. These were determined from the solar position procedure mentioned above.

The resulting estimates of accumulated incoming solar radiation over a 5-year period is shown in Fig. 3.5 from the two stations. Hesselø has a larger amount of sunshine than Fanø (which here really means less cloud cover), and this is in accordance with what is known about the geographical variation of the Danish climate today (Larsen and Jensen, 1983). From this reference we cite that Hesselø is found to have 10 per cent more hours of sunshine than Fanø during the period 1961-71. Further, we should like to mention that the total incoming solar radiation has been measured at a station close to Copenhagen in the period 1966-76. Here an annual average of 1018,5 kWh/m^2 was found, corresponding to 18.3 GJoule/m^2 for a 5-year period. The figure indicates little if any trend at all, but a variability between the different 5-year averages of 10-20 per cent. Hesselø has the highest variability which is consistent with its higher climatic variability expected from the discussion in section 2.

Finally, we show the power spectra of the daily solar radiation at Fanø and Hesselø. As for the temperature spectra (Fig. 3.4) the Hesselø spectrum shows less energy at frequencies larger than one year^{-1} than the Fanø spectrum while the situation is the opposite for lower frequencies.

3.3 Variation in wind energy potential

Both on Hesselø and Fanø the wind speeds are observed subjectively in terms of a wind force estimated from the effect of the wind in nature. The Hesselø series is the simplest one to interprete because

a) the wind was observed on the Beaufort scale from start to end, see Table 3.1,

b) teams of observers were constantly present establishing a continuous concensus on use of the scale, and

c) Hesselø is surrounded by water uniformly in all directions, compare Fig. 2.3, ensuring that the surroundings have not changed over time. This again makes it simpler to establish a concensus on use of the scale as well as making corrections unncessary for gradual changes of vegetation etc. around the station.

We have translated the observed Beaufort values to wind speed in meter/sec, using the mean values of wind speeds for each Beaufort class, compare Table 3.1. The only non-simple characteristic of the time series of wind from Hesselø is

1. until 1908 class 12 was not used in the Beaufort scale. However, from Table 3.1 is seen that this is quite unimportant,

2. until 1971 the winds were observed five times a day, thereafter only three times a day, compare Table 2.2. For the last 10 years of the series there are no proper night time observations of wind. However, since the diurnal variation at Hesselø is small owing to the maritime nature of the station, compare Fig. 3.1, and since only the last 10 years of the series is influenced by the changed times of observation we did not try to adjust the data for these changes.

For a number of reasons the Fanø data are considerably more complicated to interprete than the Hesselø series. As described in section 2 the serious problems with the Fanø wind data were one of the main arguments for choosing a lighthouse station like Hesselø as our second station.

The problems of the Fanø wind data can be summarized as follows

a) Before 1911 a 7-category wind force scale was used, and thereafter the Beaufort scale was used,

b) the station was attended by a single person at a time, and while each observer appeared to be consistent in his own method of observing, there are large differences in the frequency distribution of the observed winds reported by different observers (Peterson, 1983, Peterson and Larsen, 1984b),

Tabel 3.1. The Beaufort scale for wind force and wind speed equivalence (Larsen and Jensen, 1983).

Beaufort No.	Description	Velocity equivalent at a standard height of 10 m above open flat ground			Specification of estimated speed over land	Specification of estimated speed over "sea"
		Knots	m/s	km/h		
0	calm	< 1	0-0.2	< 1	smoke rises vertically	the sea is like a mirror
1	light air	1-3	0.3-1.5	1-5	wind direction shown by smoke drift but not by wind vanes	ripples are formed with appearance of scales, but without foam crests
2	light breeze	4-6	1.6-3.3	6-11	wind felt on face; leaves rustle; ordinary vanes moved by wind	small wavelets, still short but more pronounced; crests have a glassy appearance and do not break
3	gentle breeze	7-10	3.4-5.4	12-19	leaves and small twigs in constant motion; wind extends light flag	large wavelets; crests begin to break; foam og glassy appearance; perhaps scattered white horses
4	moderate breeze	11-16	5.5-7.9	20-28	raises dust and loose paper; small branches are moved	small waves, becoming longer; fairly frequent white horses
5	fresh breeze	17-21	8.0-10.7	29-38	small trees in leaf begin to sway, crested wavelets form on inland water	moderate waves, taking a more pronounced long form; many white horses are formed (chance of some spray)
6	strong breeze	22-27	10.8-13.8	39-49	large branches in motion; inconvenience felt when walking against the wind	large waves begin to form; the white foam crests are more extensive everywhere (probably some spray)
7	near gale	28-33	13.9-17.1	50-61	whole trees in motion; inconvenience felt when walking against the wind	sea heaps up and white foam from breaking waves begins to be blown in streaks along wind direction
8	gale	34-40	17.2 - 20.7	62-74	breaks twigs off trees; generally impedes progress	moderately high waves of greater length; cages of crests begin to break into the spindrift. The foam is blown in well-marked streaks along wind direction
9	strong gale	41-47	20.8-24.4	75-88	slight structural damage occurs (chimney-pots and slates removed)	high waves; dense streaks of foam along wind direction; crests of waves begin to topple, tumble and roll over; spray may affect visibility
10	storm	48-55	24.5-28.4	89-102	seldom experienced inland; trees uprooted; considerable structural damage occurs	very high waves with long overhanging crests; foam in great patches is blown in dense white streaks along the wind. On the whole sea surface takes a white appearance, tumbling of the sea becomes heavy and shocklike; visibility affected
11	violent storm	56-63	28.5-32.6	103-117	very rarely experienced; widespread damage	exceptionally high waves; the sea is completely covered with long white patches of foam lying in the wind direction; the edges of the waves are blown into froth; visibility affected
12	hurricane	≥ 64	≥ 32.7	≥ 118		the air is filled with foam and spray; sea is completely white with driving spray: visibility is very seriously affected

c) the station is situated on the east side of Fanø meaning that the bulk of the island influences the wind from westerly directions (see Fig. 2.3), and

d) the station has been moved around in the surroundings of the town of Nordby with changing observers (again compare Fig. 2.3), and while the influence on parameters like temperature, pressure, rain, and cloud cover probably is small, the influence on wind speed may be appreciable.

Most of these effects are quite difficult to evaluate today. However, we have established a translation between the 7- and Beaufort scales based on the instruction manuals to the observers and on wind distributions noted by one observer who observed both in the 7- and Beaufort scales (eterson, 1983, Peterson and Larsen, 1984b). Hereby we can at least present formally the winds for the whole period in meter/sec.

The records of mean speeds during a 5-year period for Hesselø and Fanø are presented in Fig. 3.7. To this figure we may comment that the wind distributions at Fanø in the 1930'es and first part of the 1940'es appear to be quite inconsistent with distributions in the rest of the series, and therefore the very low values here (Fig. 3.7) are probably dependent of the observer. We also note that the Fanø values are consistently lower than the Hesselø ones. This, however, is consistent with the different roughness surroundings of the two stations.

Owing to the difficulties with the Fanø wind data we shall concentrate on the information from Hesselø in the following.

For an evaluation of the wind energy potential the frequency distribution function of the wind speed must be known. Here the Weibull distribution is by far the one mostly accepted

$$F(U) = \left(\frac{k}{A}\right)\left(\frac{U}{A}\right)^{k-1} \exp\left(\left(-\frac{U}{A}\right)^{k}\right) \quad , \tag{4}$$

where U is the wind speed, k and A are the two parameters characterizing the Weibull distribution. A is related to the mean speed through

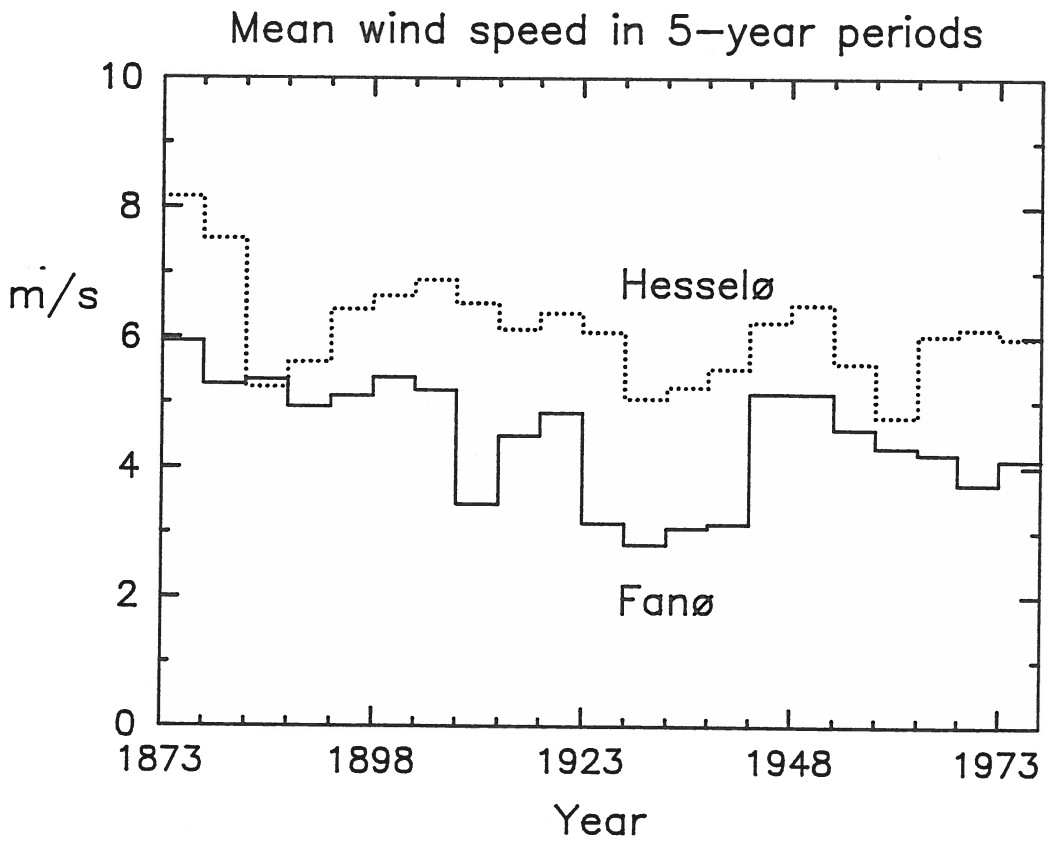

Fig. 3.7. Five-year mean speeds at Fanø and Hesselø based on the raw observations.

$$\bar{U} = A\Gamma(1 + 1/k) \quad , \tag{5}$$

where Γ is the Gamma function.

The wind distributions for areas like Denmark are characterized by k-values slightly less than 2. From Eq. (5) is seen that the parameter A therefore is very close to $\bar{U}$, generally 10 per cent larger than $\bar{U}$.

We determined the A and k parameters for our Beaufort observations by comparing the probability mass in each Beaufort interval, compare Table 3.1, according to the Weibull distribution with the observed frequencies. The (A, k) values were determined by the least square method. The resulting Weibull distribution for the total period of data at Hesselø is shown in Fig. 3.8 together with the corresponding integral probability.

The variability of the wind distributions is illustrated in Figs. 3.9 and 3.10. Figure 3.9 shows the Weibull distributions for each of the individual 5-year segments of the series. Figure 3.10 shows series of the A and k-parameters determined from the monthly wind distributions. From Fig. 3.10 we note quite a large variability in the monthly values of both k and A in which as remarked above the latter closely corresponds to the mean speed. Also we note that the value of k tends to be smaller than the "typical value of slightly less than 2" cited above. This is not an artifact of the estimation technique since we tested also other techniques with similar results, for example, we used the moment method where we used the first and the third moment of the distributions to determine A and k. We rather believe it to be a result of the subjective method of observation since the observers tend to overestimate the high wind speeds. This is a fact that clearly reflected in the frequency distributions in which the medium high wind speeds are less represented than in the Weibull distributions whereas the very high wind speeds are overrepresented.

To derive the wind energy potential derivable from the wind energy distributions discussed above, we first note the the simplest type of arguments indicates that the available power is proportional to U^3, since the kinetic energy available per m^2 per second equals $\frac{1}{2}(\rho_{air} \cdot u)u^2$.

In Fig. 3.11 we show the variation of the 5-year mean value of u^3 as well as the corresponding standard deviations both derived from the Weibull

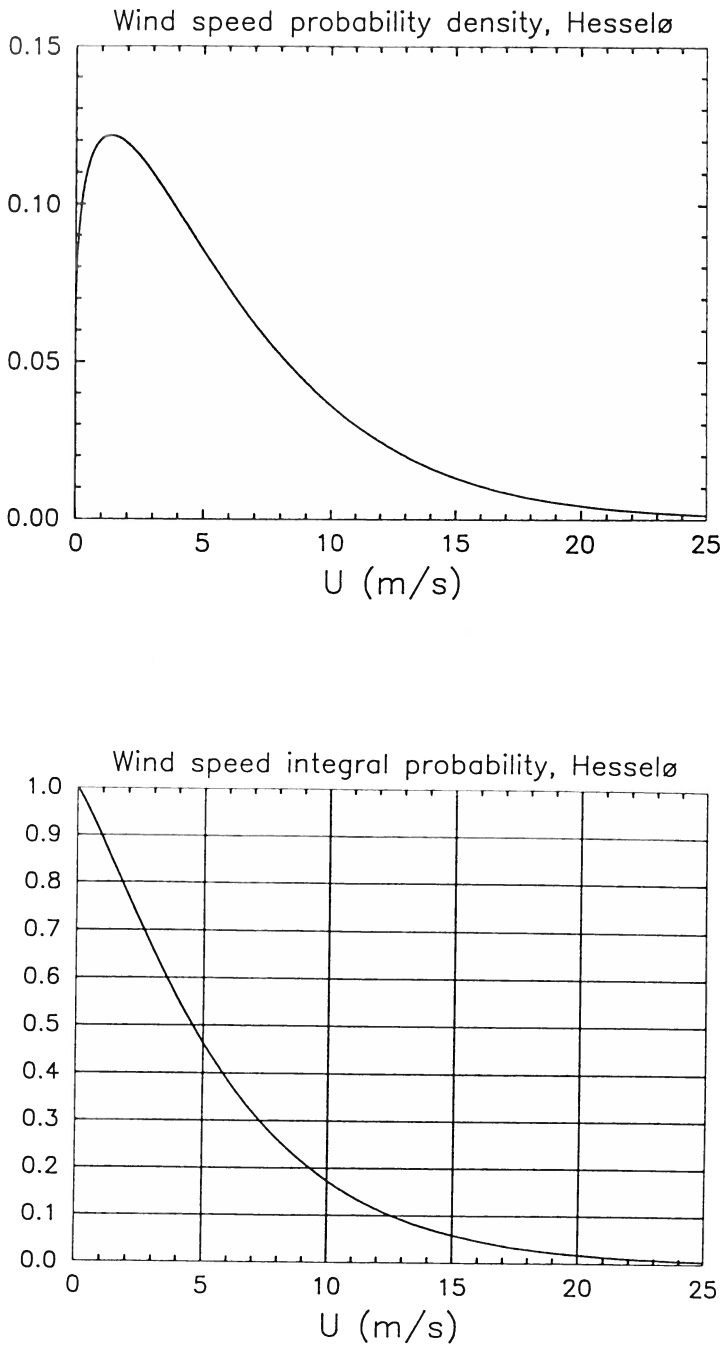

Fig. 3.8. Weibull distributions for the Hesselø series. Both the frequency and integral probability are shown.

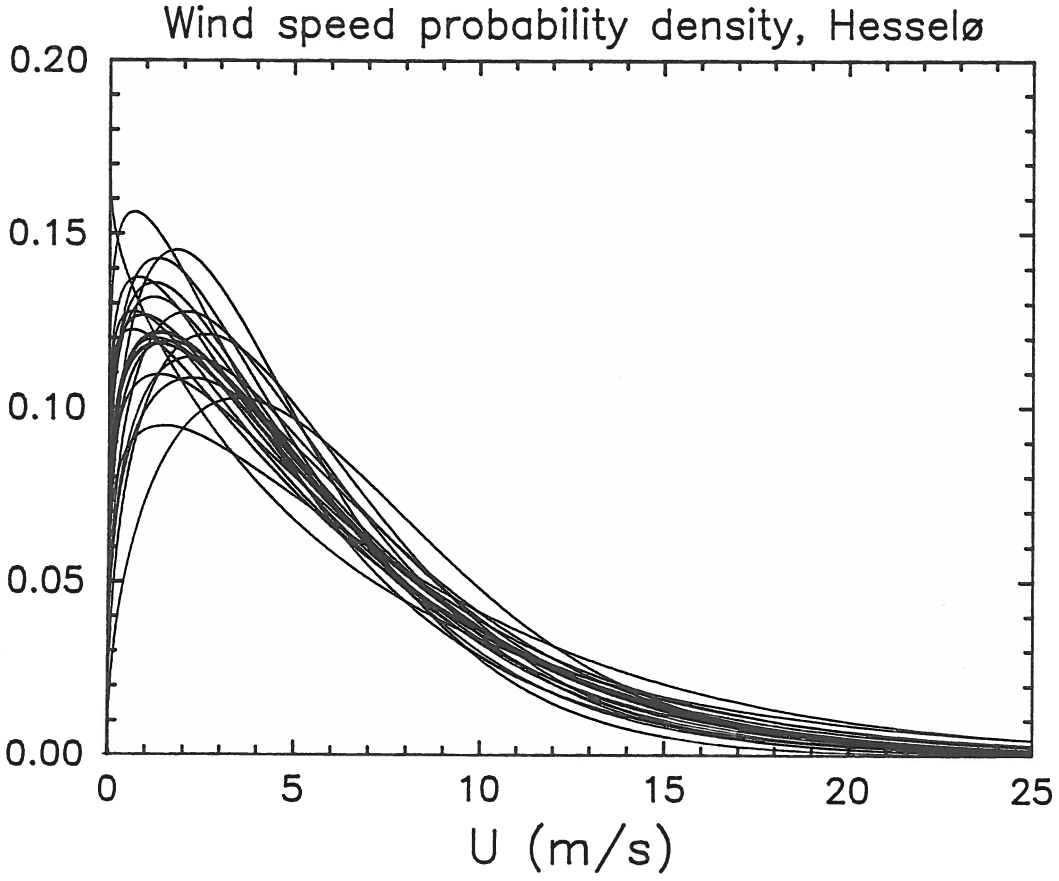

Fig. 3.9. The 21 five-year Weibull distributions for the Hesselø data. The distribution is shown with a heavier line corresponding to the total series as given in Table 3.6.

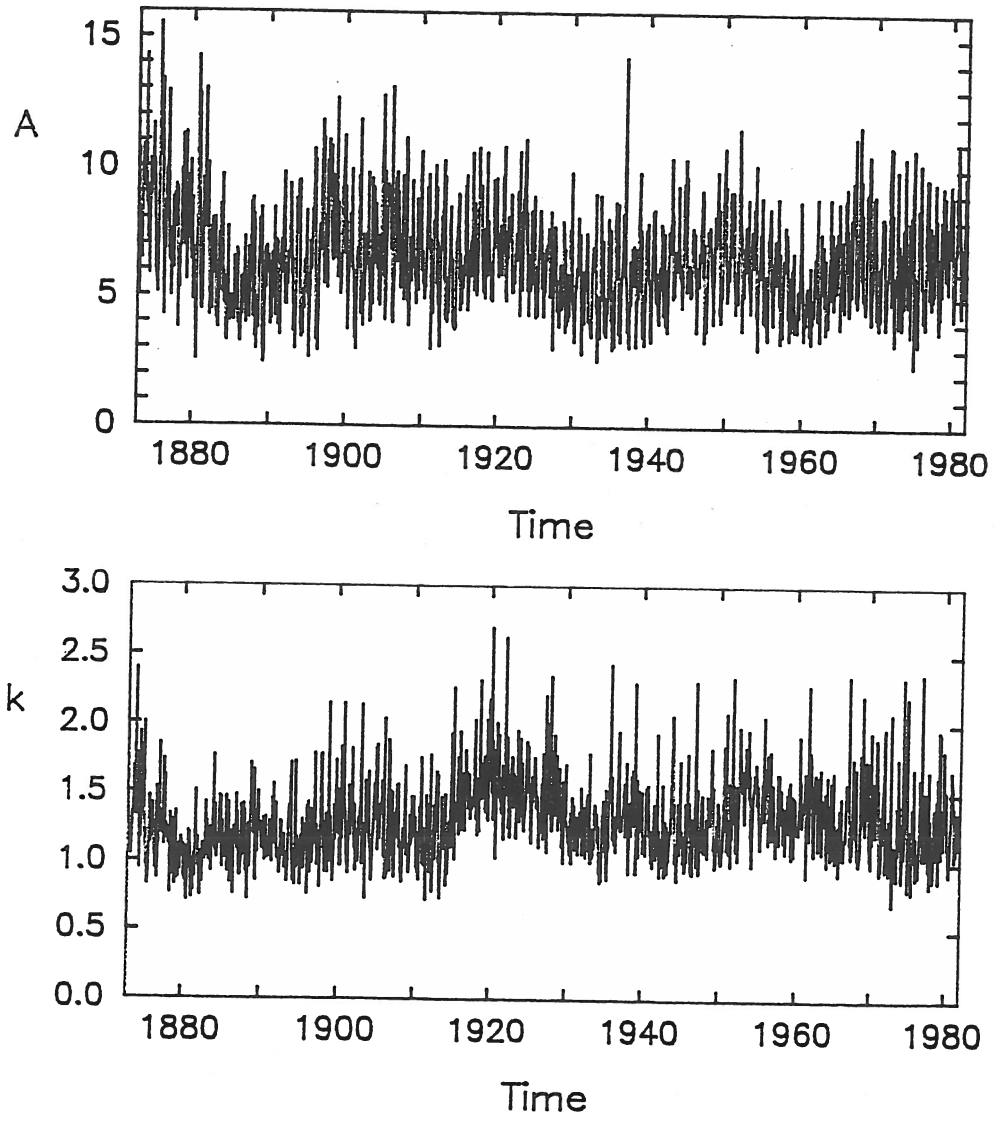

Fig. 3.10. The A [m/s] and k-parameters for Weibull distributions associated with each month in the duration of the Hesselø series.

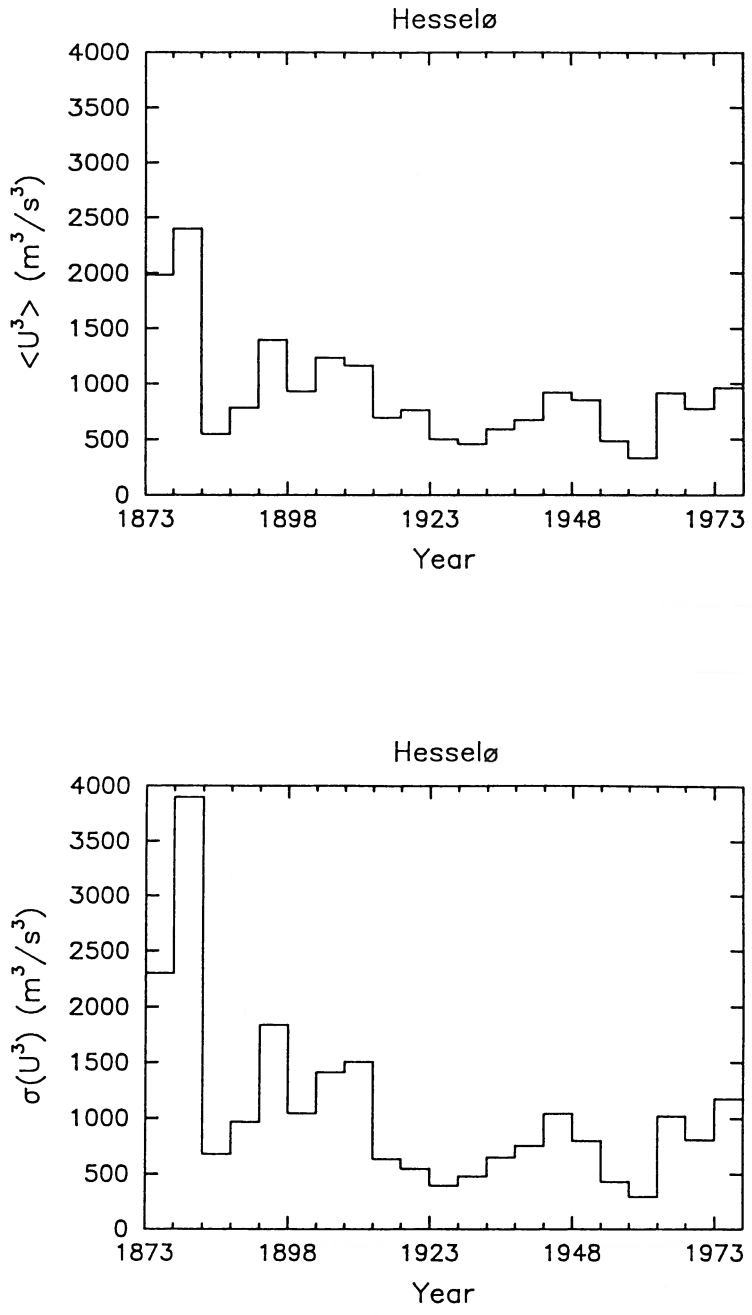

Fig. 3.11. The 5-year mean values of U^3 with corresponding standard deviations. The values are estimated from the 5-year Weibull functions shown in Fig. 3.9.

distributions shown in Fig. 3.9. The variability between the individual 5-year mean values is seen to be of the order of ± 40 per cent around the long-term mean. Apart from being of interest in the wind energy context, the curves in Fig. 3.11 are of interest also in connection with discussions regarding pollution of the regional seas, since U^3 is the wind energy available also for mixing of the mixed layer in the ocean. The curves in the figure can be translated therefore into the climatic variation of the mixed-layer depth in the Kattegat and neighbouring waters, all other parameters being the same.

For a more accurate description of the wind energy potential we turn to the work performed at Risø National Laboratory under the EEC project "European Wind Atlas" for the European Community countries which has been conducted since 1981 (Petersen and Troen, 1986). Rather than the simplistic u^3-argument from the above a real power curve is used here, i.e. the relation between power production and wind speed. The power curve is shown in Fig. 3.12 and corresponds to a usual small Danish windmill with 55 kW rated power and a hub height of 24 m. With the power, $P(U)$, as given in Fig. 3.12 we can now obtain the 5-year mean wind energy production E from

$$E \sim \int_0^\infty P(U)\, F(U) dU \quad , \tag{6}$$

where $F(U)$ is the 5-year Weibull distribution functions. These functions are shown in Fig. 3.9 with the addition that the distribution functions shown in Fig. 3.9 pertain to 10 m above water surface. The distribution functions $F(U)$, used in Eq. (6) were obtained from the former by extrapolating to hub height (24 m) using the formalism described in Petersen et al. (1987) with a water roughness equal to 0.2 mm which was found to describe best over-water situations in the European Wind Atlas study previously mentioned. We note that rather than the simple U^3-argument the use of Eq. (6) to some extent reduces the sensitivity of E to the frequency of extreme winds since the power curve used is flat for $U > 15$ m/s. This is fortunate since the fairly low values of the k-parameters in the observations indicate difficulties of the observers in distinguishing between the different high-wind Beaufort categories, as discussed above.

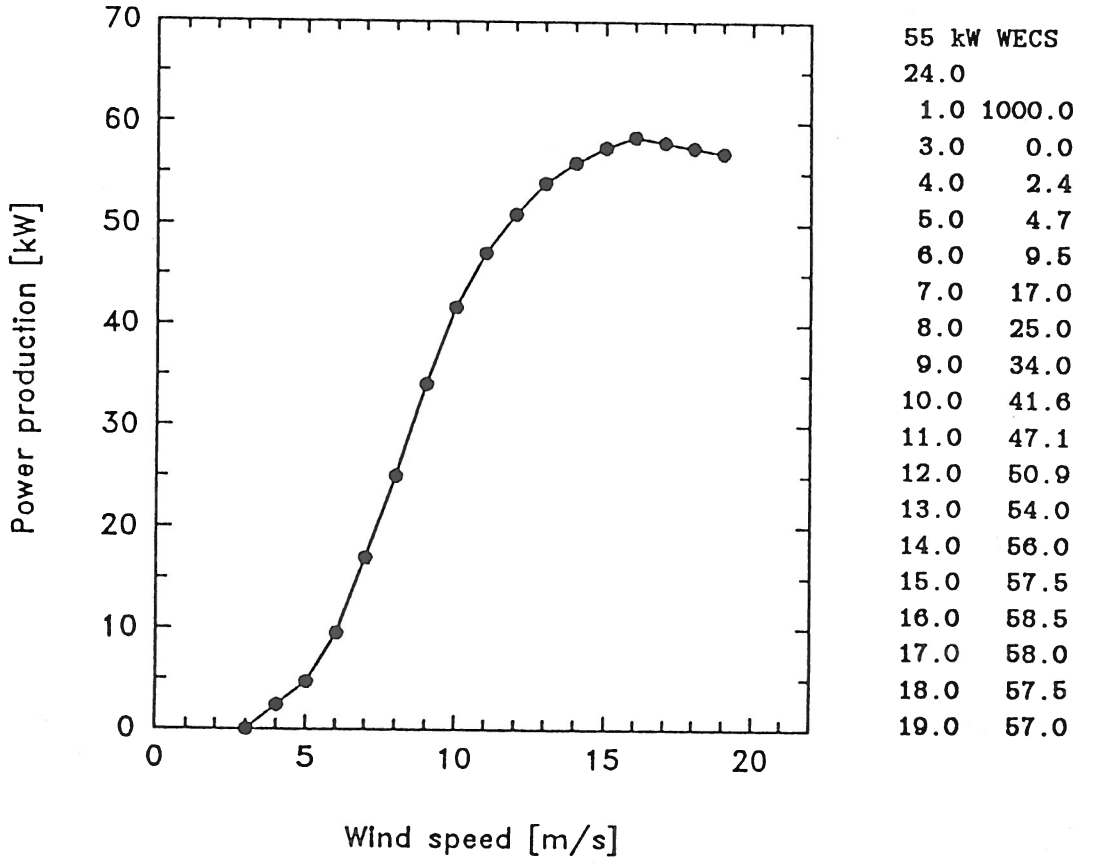

Fig. 3.12 Power curve of a 55-kW wind turbine used to evaluate the climatic variations of the wind energy potential depicted in Fig. 3.11. The curve is taken from Troen et al. (1987).

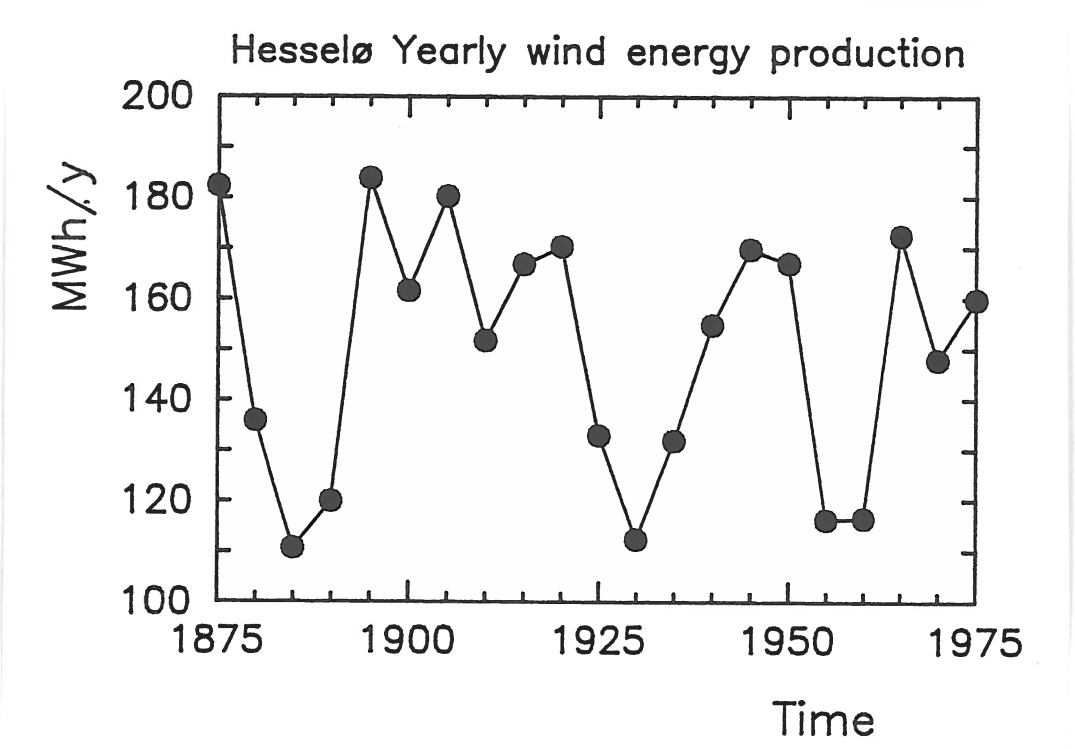

Fig. 3.13. Average yearly power production for consecutive 5-year periods based on the power curve in Fig. 3.12 and the Hesselø data. The value relevant for a given 5-year period is plotted in the start of the period.

Figure 3.13 shows the yearly mean production based on consecutive 5-year data determined as described above. Little trend if any can be distinguished, but a variability of about ± 30 per cent is clearly seen around the long-term mean. At the same time it appears from the figure that production estimates based on wind data from the last 10 years or so will be very close to the long-term average. Also it is interesting to note that while a decreasing trend is obvious in the mean speed of Fig. 3.7, this tendency is completely swamped by the variability in Fig. 3.13. Finally, Fig. 3.14 shows the wind spectra for Fanø and Hesselø. The yearly peak seems a bit small at Fanø, but apart from this the Fanø spectrum tracks the Hesselø spectrum remarkedly well.

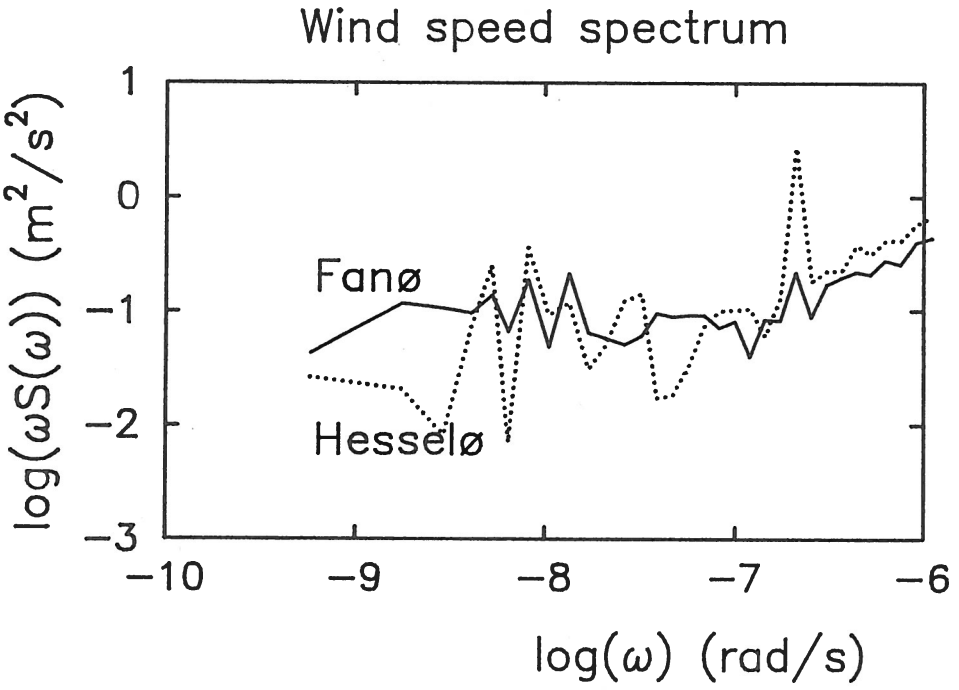

Fig. 3.14. Power spectra of the daily mean winds on Fanø and Hesselø.

3.4 Variability of atmospheric dispersion

To describe the climatic variability of atmospheric dispersion we shall consider two simple models, the Gaussian plume model and the simple box model. Both models are depicted in Fig. 3.15. The ground concentration around an elevated point source is given by

$$\frac{\chi}{Q'} = \frac{1}{\pi \sigma_y \sigma_z U} \exp\left[-\left(\frac{y^2}{2\sigma_y^2} + \frac{h^2}{2\sigma_z^2}\right)\right] \quad , \tag{7}$$

where χ is the concentration, Q' the source strength, h the height of source (h is constant if we consider a non-buoyant gas), U is the mean speed, y the lateral coordinate while σ_y og σ_z are the standard deviation of the plume concentration, which is a function of downwind distance from source and thermal stability of the boundary layer. The equation applies for $\sigma_z + h < H$, where H is the inversion height. A particular simple expression appears if we consider the crosswind-integrated concentration χ_{CWI} and neglect the influence of H

$$\frac{\chi_{CWI}}{Q'} = \sqrt{\frac{2}{\pi}} \frac{1}{\sigma_z U} \exp\left(-\frac{h^2}{2\sigma_z^2}\right) \quad . \tag{8}$$

Here again we can ask for the maximum

$$\frac{\chi_{CWI}}{Q'}\Big|_M = \sqrt{\frac{2}{\pi}} \frac{1}{\sigma_z(x', stab) \cdot U \cdot \mathrm{e}} \tag{9}$$

where we emphasized that σ_z is a function of stability ($stab$) and downwind distance x'. The latter is determined by

$$\sigma_z^2(x', stab) = h^2 \quad . \tag{10}$$

The well-mixed simple box model is also illustrated in Fig. 3.15. While the Gaussian plume model is intended for decribing dispersion of a singular

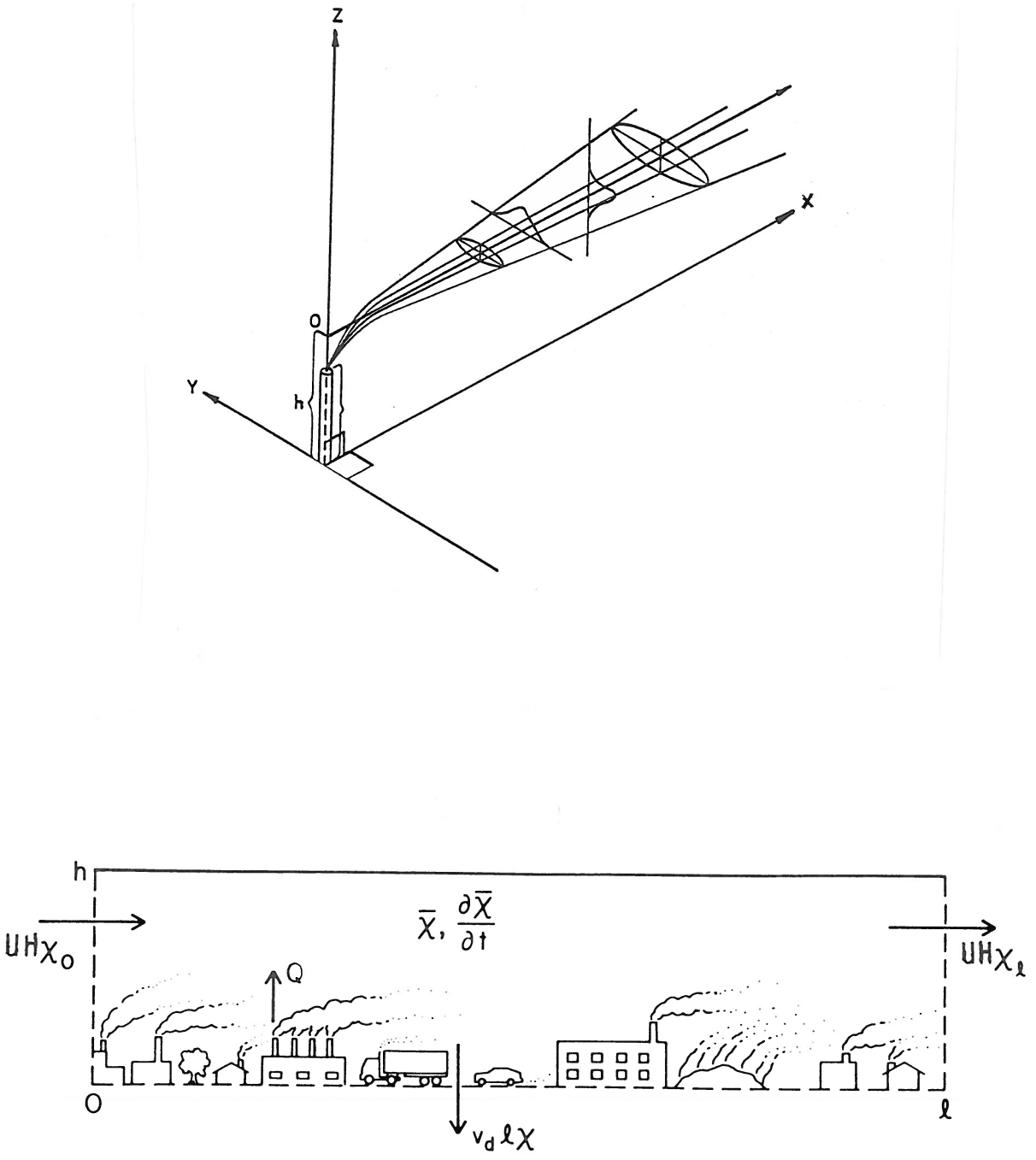

Fig. 3.15. Illustration of dispersion from 1) a single point source by a Gaussian plume model, 2) extended area sources described by a well-mixed box model.

point source, the box model is better suited to describe developments of concentration for extended areas with a multitude of sources and sinks.

Based on Fig. 3.15 a simple mass balance yields

$$H \cdot \ell \cdot \frac{\partial \bar{\chi}}{\partial t} = \ell \cdot Q + UH\chi_0 - UH\chi_\ell - \ell v_d \bar{\chi} \quad , \tag{11}$$

where $\bar{\chi}$ is the spatially averaged concentration, Q is the average area source strength. As in Eq. (7) H is the inversion height while ℓ is the horizontal extent of our polluted area. Assuming that the vertically averaged concentration χ varies linearly with the downwind distance, we can rearrange Eq. (11) to read

$$\frac{\partial \bar{\chi}}{\partial t} = \frac{Q}{H} - 2\bar{\chi}\frac{U}{\ell}\left(1 - \frac{\chi_0}{\bar{\chi}}\right) - \frac{v_d}{H}\bar{\chi} \quad . \tag{12}$$

Assuming steady state conditions, $v_d \sim 0$ and $\chi_0/\bar{\chi} << 1$ we finally obtain

$$\frac{2\bar{\chi}}{\ell Q} = \frac{1}{UH} \quad . \tag{13}$$

From both Eq. (9) and Eq. (13) we see that the resulting relative concentration is inversely proportional to U and a height scale that specifies vertical mixing. Both σ_z and H are known to depend on stability. Here it is most complicated to determine H, since it is generally known that it depends not only on the present situation, but rather has to be determined by a rate equation. However, for many practical purposes a simple direct relationship with stability is used, originally due to Klug (1969). At present we shall use Eq. (13) rather than Eq. (9) to estimate the climatic variability of dispersion, here taken as the variability of $\bar{\chi}/Q$. The reason is that Eq. (9) involves an arbitrary source height as well as variation in space, both given by Eq. (10). Of the variables in Eq. (13) our time series already contain the wind speed, U, and therefore we only have to derive stability and thereby H. We shall follow the philosophy of section 3.2 in which solar radiation was determined from the observations of cloud cover. Numerous schemes

were developed to determine stability from solar radiation. In the following we shall use one owing to Turner (1964), who derived dispersion stability classes using a combination of cloud clover, solar altitude and wind speed. We used the Turner (1964) scheme as follows. Since we have no information about the height of cloud ceiling we simplified the scheme always assuming the ceiling to be less than 7,000 ft.

A simplified wind speed index was used that could be computed from the Beaufort observations

Beaufort	0	1	2	3	≥ 4
I_w	0	1	2	3	4

The Turner (1964) insulation classification numbers are

$I_s = 0$ for night time observations
$I_s = 1$ for $0° < \varphi \leq 15°$
$I_s = 2$ for $15° < \varphi \leq 35°$
$I_s = 3$ for $35° < \varphi \leq 60°$
$I_s = 4$ for $60° < \varphi \leq 90°$

where φ is the solar altitude computed as in section 3.2.

Knowing I_s and the cloud cover, $N(0-10)$, which is an observed quantity, the Turner net radiation index I_N is found from

Table 3.2. I_N versus N and I_s

$I_s \setminus N$	0	1	2	3	4	5	6	7	8	9	10
0	-2	-2	-2	-2	-2	-1	-1	-1	1	-1	0
1	1	1	1	1	1	1	1	1	1	1	0
2	2	2	2	2	2	2	2	2	2	2	0
3	3	3	3	3	3	3	1	1	1	1	0
4	4	4	4	4	4	4	2	2	2	2	0

From I_W and I_N we can determine next the stability index I

Table 3.3. I versus I_N and I_W.

$I_W \setminus I_N$	4	3	2	1	0	-1	-2
0	1	1	2	3	4	6	7
1	1	2	2	3	4	6	7
2	1	2	3	4	4	5	6
3	2	3	4	4	4	4	5
4	3	4	4	4	4	4	4

The below listing shows the relation between the Turner stability index I (1-7) and the often used Pasquill-Turner classes (A-G). Also shown are the inversion heights pertaining to each stability class according to Klug (1969) and the frequency of classes obtained from 20 years of Risø data.

Table 3.4. Turner stability index, I, Pasquill-Turner class, stability, inversion height, H. Also shown is the frequency of occurrence from the tower Risø data of Pasquill-Turner classes.

I	Pasq-Turner Class	Stability	$H[m]$	Frequency at Risø
1	A	very unstable	1,500	2 %
2	B	unstable	1,500	2 %
3	C	weakly unstable	1,000	7%
4	D	neutral	500	70 %
5	E	weakly stable	200	10 %
6	F	stable	200	9%
7	G	very stable	200	

Based on the procedure outlined above we have computed the stability distribution at Fanø and Hesselø. The 5-year mean frequencies for neutral (D), stable (E+F+G) and unstable (A+B+C) are shown in Fig. 3.16. Both

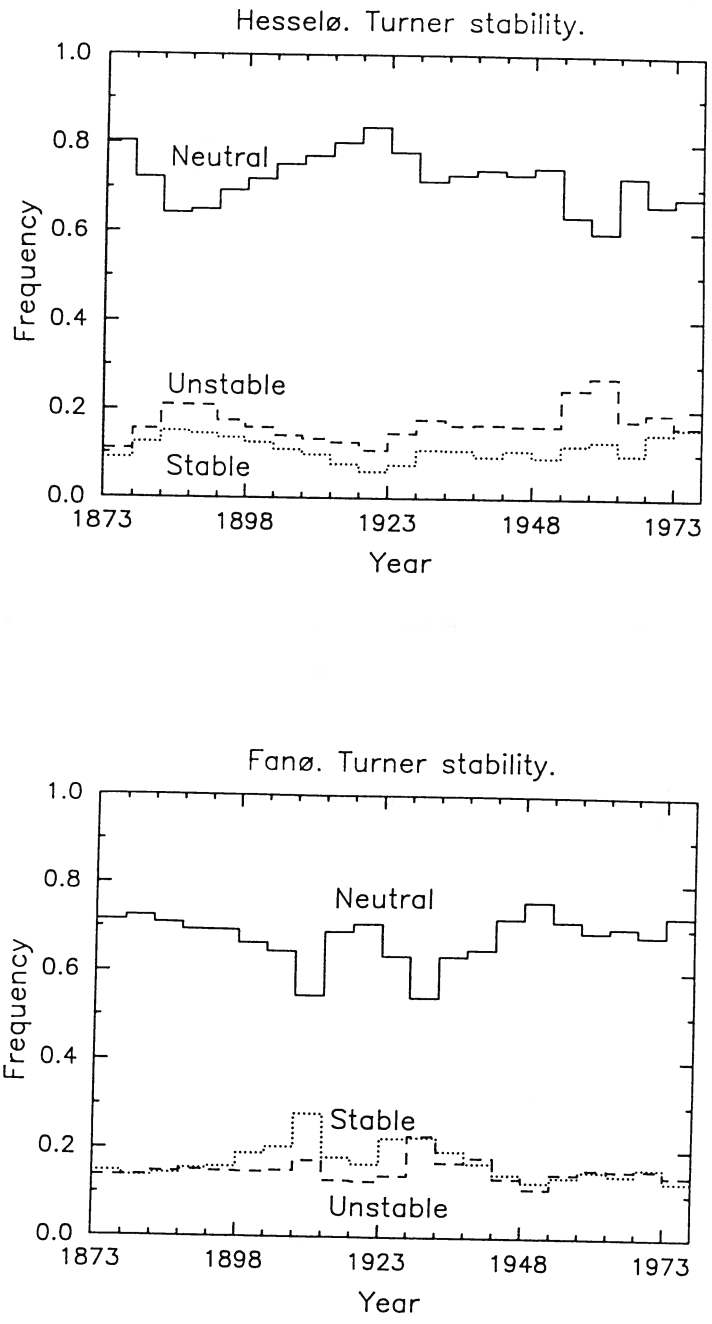

Fig. 3.16. Five-year mean frequencies of stability classes at Hesselø and Fanø. Class D is neutral while the sum of frequencies for classes E,F, and G is stable and the sum of classes A,B, and C is unstable.

figures in Fig. 3.16 show slightly larger frequency of unstable and smaller frequency of stable classes than depicted in Table 3.4. An obvious reason for the Fanø data is that this series contains no observations between 2100 and 800 hours, compare Table 2.2. Hereby the night data are underrepresented in the Fanø statistics. The reason for the deviation of the Hesselø data is less transparent. It is worthwhile summarizing the background of stability schemes like that of Turner: the basic property for parameterizing atmospheric dispersion is the boundary layer turbulence. This turbulence is best evaluated from estimates of the vertical turbulent heat flux and wind speeds. For surfaces with known thermal and albedo characteristics an approximate relation can be found between net radiation at the ground (and thereby solar altitude and cloud cover) and the turbulent heat flux. These relationships are utilized in empirical schemes like that of Turner but pertain only to land surfaces. The stability classes we report from Hesselø are therefore not real. They rather report the stability classes we would find if Hesselø were a land station with the same cloud cover and wind observations. In a way this is quite acceptable, since we are more interested in the climatic variation of dispersion over a such land surface than over a sea surface. However, subtle differences in cloud cover over the sea and over land might slightly change the stability class frequency reported from Hesselø compared to the "typical Danish standard" as shown in Table 3.4, which pertains to land surfaces. By way of example may be mentioned that while most convective activity over land occurs in the daytime during the warm season much convection may occur over sea at night in winter.

Finally, we should comment that in the Fanø series periods with a relatively small frequency of neutral conditions clearly correspond to the periods during which velocity is reported to be very small and somewhat doubtful, compare the discussion in section 3.3.

We have not tried to correct for any of the uncertainties in the stability statistics of Fig. 3.16 described above since too little information is available.

In Fig. 3.17 we show the 5-year mean values of the normalized concentration for Hesselø as given by Eq. (13) together with the corresponding relative standard deviations of the instantaneous concentrations around their respective mean values. Note that from Eq. (13) we have

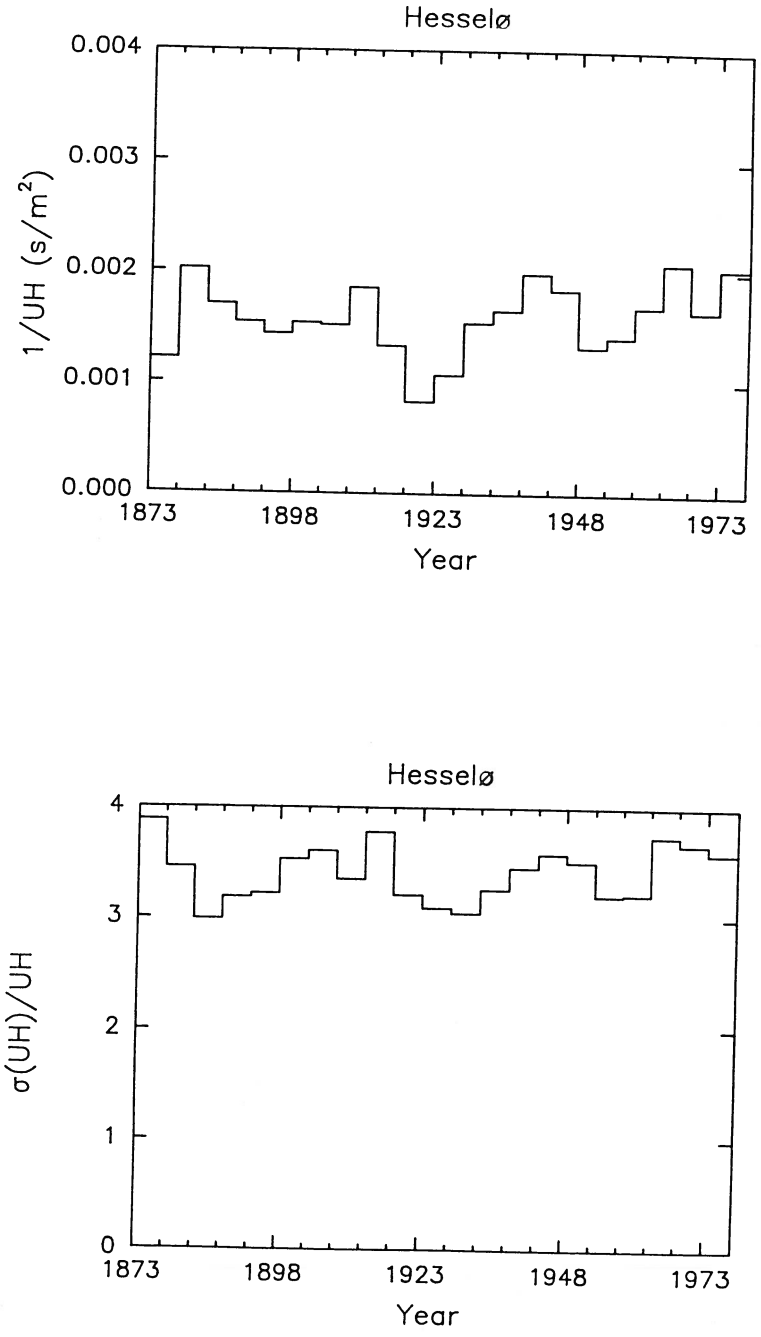

Fig. 3.17. Five-year normalized mean concentration for Hesselø with associated standard deviations, σ. The concentrations are presented in terms of the mean values of $1/UH$, in which U is the velocity and H the inversion heights, compare Eqs. (13) and (14).

$$\frac{\sigma(\chi)}{\bar{\chi}} = \frac{\sigma(UH)}{UH} \quad . \tag{14}$$

For completion the corresponding values are shown for Fanø in Fig. 3.18. However, we have little confidence in Fig. 3.18 due to the problems of wind speed observations on Fanø.

It is seen that the 5-year mean concentrations of the Hesselø data vary about ±50 per cent around the long-term mean value and that the corresponding standard deviation is relatively constant being about 350 per cent around each 5-year average with a variability of approximately 10 per cent.

In connection with air-pollution regulations it is common to formulate standards in terms of how often a concentration averaged over a certain time (generally 10 min to 1 hour) may exceed a certain level. In general, the one per cent percentile is used. We shall therefore try to relate our results to this approach.

As depicted in Fig. 3.15 our model situation corresponds to measurements in a city where the sensor is exposed to dispersion from a huge amount of different sources under variable atmospheric aconditions. The frequency distribution of χ for such a situation is normally found to be close to a longnormal distribution (Larsen, 1969, Larsen and Petersen, 1974)

$$p(\chi) = \frac{1}{\chi s\sqrt{2\pi}} \exp\left(\frac{1}{2s^2}(ln\chi - \mu)^2\right) \quad , \tag{15}$$

where the geometric mean, μ, and the standard geometric deviation, s, is related to the mean value, $\bar{\chi}$, and the standard deviation, σ, through

$$\begin{aligned} s^2 &= \quad ln(\sigma^2/(\bar{\chi}^2+1)) \\ \mu &= ln(\bar{\chi}/(\sigma^2/(\bar{\chi}^2+1)^{1/2}) \quad . \end{aligned} \tag{16}$$

Having estimated s and μ, the percentile of the order p can be determined from

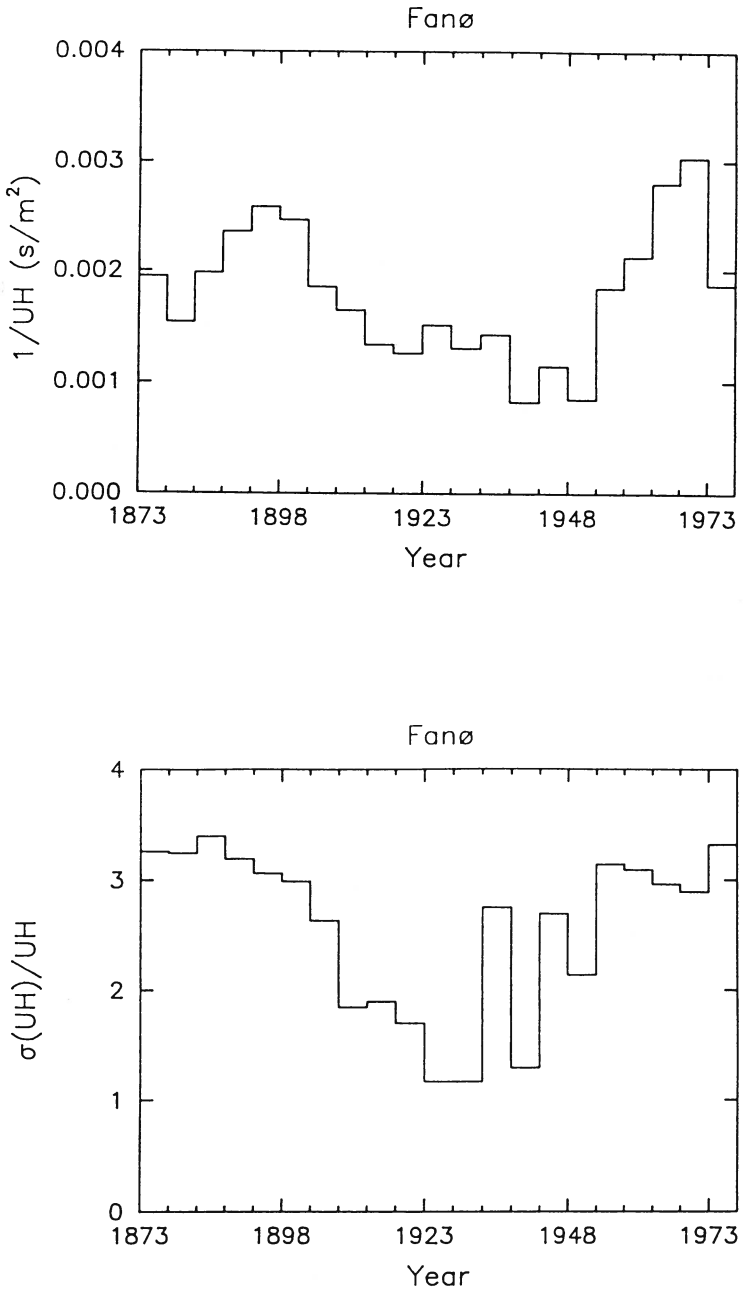

Fig. 3.18. The same concentration estimates as in Fig. 3.17 but for Fanø.

$$\chi_p = e^{\mu + y_p s} \quad , \tag{17}$$

where y_p is the corresponding percentile for a standard normal distribution, i.e.

$$\begin{aligned} y_{0.01} &= 2.33 \\ y_{0.1} &= 0.128 \end{aligned}$$

In Fig. 3.19 we show the $\bar{\chi}$-disribution on Fanø and Hesselø determined as the number of occurrences of $(UH)^{-1}$ for the total series. As presented versus $\log(UH)$ the distributions would have looked like normal ones if $\bar{\chi}$ were lognormal. Obviously, the distributions in Fig. 3.19 look too skew $(UH)^{-1}$ to be considered lognormal.

A reason for this may be that our modelling χ by Eq. (13) is too simple to match the real world. One obvious source of additional variability is seen from Eq. (12) to be the source term Q that in the real world will vary both with times and wind direction as opposed to our model description where Q is kept constant. One could easily imagine such additional variability to force the distribution of χ closer to a lognormal than the distributions shown in Fig. 3.19. This argument can be supported by comparing the standard geometric deviation for real-pollution time series with the value from our description. From Fig. 3.17 we find $\sigma(\chi)/\bar{\chi} \sim 3.5$, which through Eq. (16) yields $s \simeq 1.6$. For large built-up areas a value of s between 2 and 3 is typical (Larsen, 1973), yielding a $\sigma(\chi)/\bar{\chi}$ between 7.3 and 90. Hence, it is obvious that we have lost a good deal of variability in our model approach. However, our mean value estimates are probably not influenced that much since we neglected the variability of the source term around a mean value. It should be added that the measured standard geometric deviation quoted above pertains to 5-min averages. This probably corresponds quite well to the implicit averaging times for the observed wind speed. The cloud cover and thereby H have even larger implicit averaging times involved.

As quoted above we found from the Hesselø data a variation of ± 50 per cent in the series between each 5-year mean concentration. Furthermore,

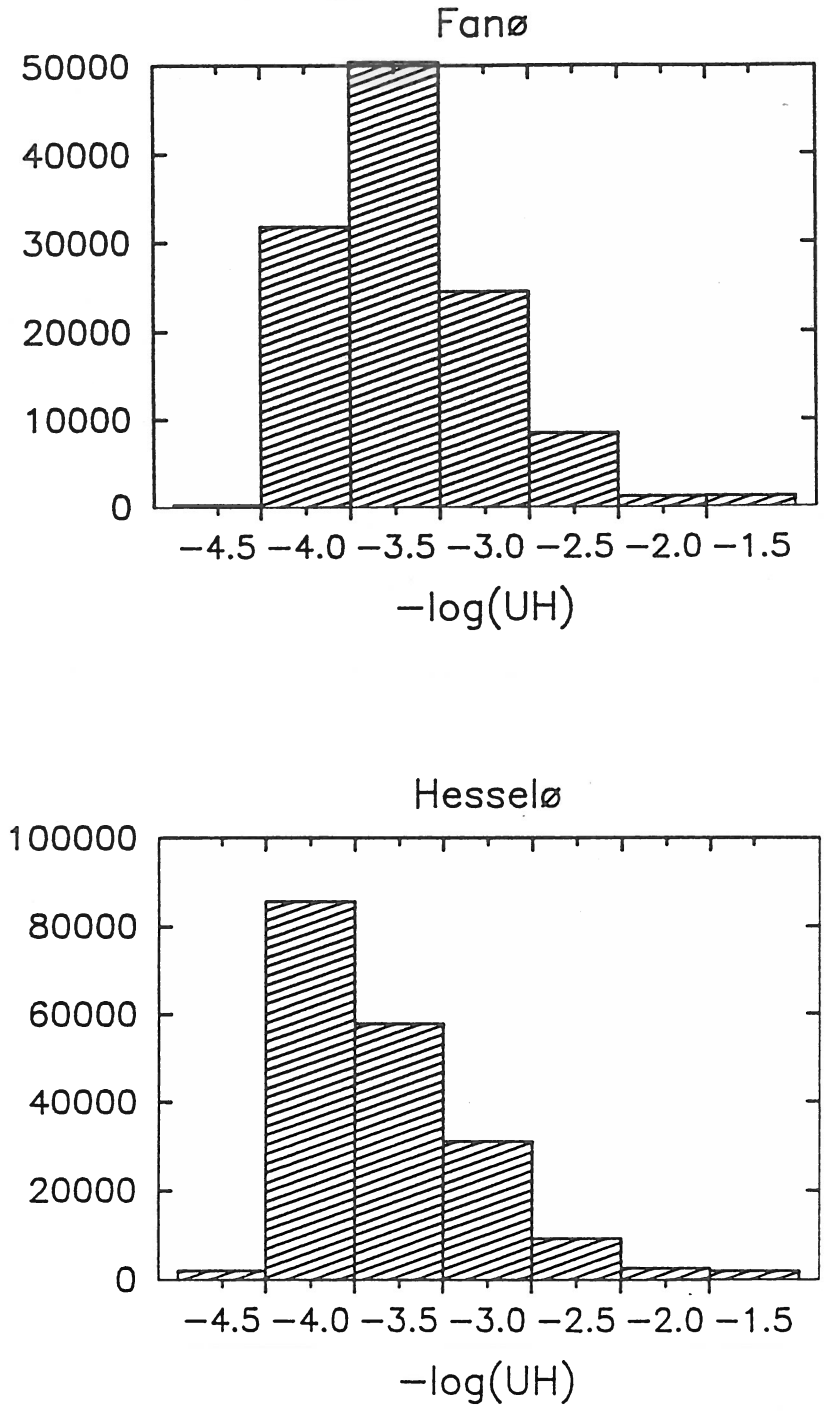

Fig. 3.19. Frequency distribution of the normalized pollution concentration $(UH)^{-1}$, compare Eq. (3.14), for Fanø and Hesselø. The distributions are presented in terms of the number of cases in each -log(UH) interval for the total series.

we found $\sigma(\chi)/\bar{\chi} \sim 3.5$ with a variability of around ± 10 per cent. Also it is seen from Fig. 3.17 that there is little if any correlation between variation of the 5-year values of $\bar{\chi}$ and $\sigma(\chi)/\bar{\chi}$. As a conclusion of this section we shall see how this kind of variability will influence the percentile value given by Eq. (3.18). We denote $\sigma(\chi)/\bar{\chi}$ by α and find by differentiating that

$$\frac{\Delta\chi_p}{\chi_p} = \frac{\Delta\bar{\chi}}{\bar{\chi}} + \frac{\alpha^2}{\alpha^2+1}\left(\frac{y_p}{s} - 1\right)\frac{\Delta\alpha}{\alpha} \quad , \tag{18}$$

which describes the variation of the p's percentile between the different 5-year periods in response to the variation in $\bar{\chi}$ and α cited above.

Assuming that our mean values are well estimated, we can either (1) use our value of α or (2) use the more realistic values cited above from Larsen (1973). With the two assumptions we obtain e.g. for the 1 per cent percentile ($y_{0.01} = 2.33$)

$$\frac{\Delta\chi_{0,01}}{\chi_{0,01}} \sim \pm 50\% \pm \begin{cases} 5\% & \sim \pm 55\%(\text{our } \alpha) \\ 10\% & \sim \pm 60\%(\text{realistic } \alpha) \end{cases} \tag{19}$$

Here we assume that $\Delta\alpha/\alpha$ is the same for the two cases since source variability is assumed not to change from one 5-year period to the next. In both cases is seen that the relative variation in $\chi_{0.01}$ is dominated by the relative variability in $\bar{\chi}$.

4 Results on humidity, precipitation and pressure

The analyses described in section 3 all aimed directly at evaluating the energy and dispersion questions central to the present project. However, the same time series can be used to study the climatic variability of a host of other parameters, e.g. the data presented for U^3 in Fig. 3.11., which show variability of ocean mixing. Together with other choices of basic temperature the heating degree-day concept employed in section 3.1, Eq. (1) can be used to evaluate the growth season for various types of vegetation. The data available on solar radiation (cloud cover), wind, temperature, humidity, and precipitation can be used to give a fairly complete description of the variation in the general conditions for plant life etc.

For these reasons and because to a certain degree data for the different parameters can be said to support and illuminate each other, we shall summarize in this section findings on the parameters not considered directly in section 3.

4.1 Humidity data from Fanø

These data were analysed in Peterson (1983) and it was generally found that the dew point temperature closely followed the development of temperature. The series was found to be contaminated with errors during the period 1940-45. But apart from this period the data were found to have a sensible appearance. Figures 4.1 and 4.2 show the variation of the annual mean, and the 30-year running mean of the dew point at the three times of observation at Fanø.

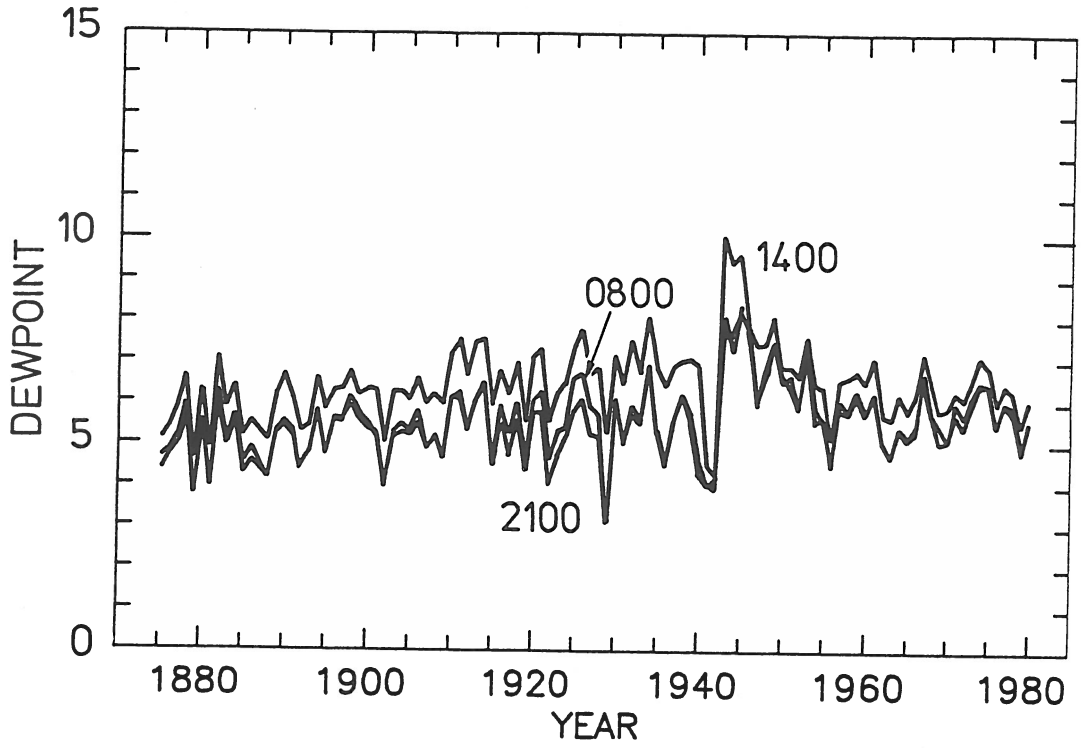

Fig. 4.1. Annual dew point on Fanø at the three times of observation (Peterson, 1983).

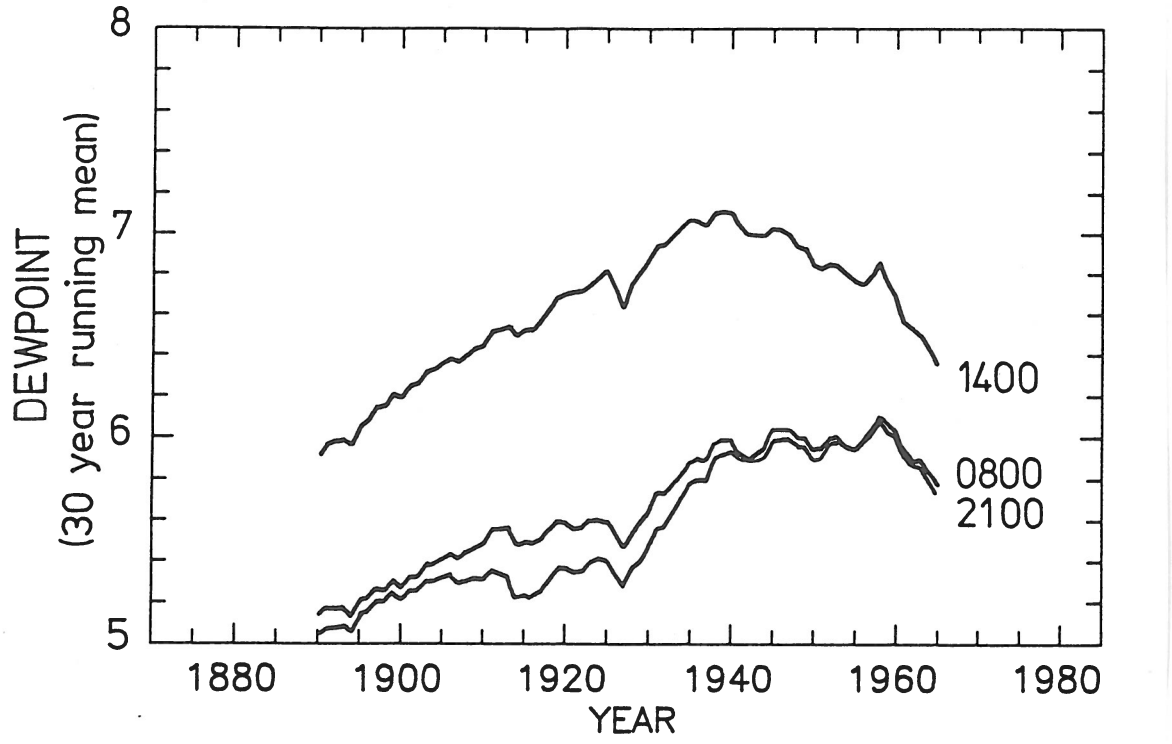

Fig. 4.2. Thirty-year running means of the data in Fig. 4.1. (Peterson, 1983).

4.2 Daily precipitation from Fanø

The precipitation for each day of the year averaged over the total series is shown in Fig. 4.3. As for the corresponding temperature shown in Fig. 3.1 the annual variation comes through clearly. However, comparison between the two figures also shows that daily precipitation is a more variable parameter around the annual mean variation than temperature. In Fig. 4.4 is shown the corresponding annual variation of the monthly mean precipitation.

Fig. 4.5 shows the annual precipitation from start to end of the series, and it is seen that also on these time scales precipitation appears as a highly variable phenomenon. Apart from the variability, precipitation, however, also shows a marked positive trend throughout most of this century as seen in Fig. 4.6 which shows the 30-year running average of the data in Fig. 4.5. In Peterson (1983) and Peterson and Larsen (1984a) is argued that this increase is due mostly to increased shower activity in accordance with tendencies found in the rest of the Nortwestern Europe as reported by Lamb (1969). This is illustrated in Fig. 4.7 that shows the 30-year running average of the number of days with precipitation larger than 20 mm/day for the six-month summer and winter periods.

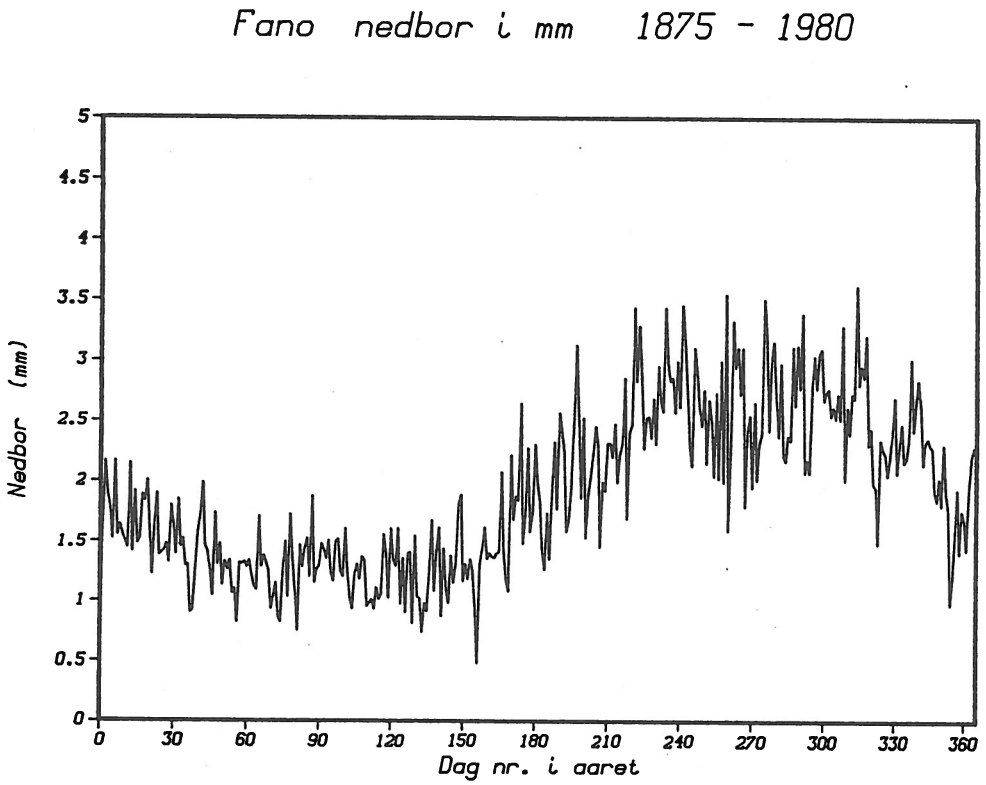

Fig. 4.3. Annual variation of daily precipitation on Fanø averaged over the length of the total series.

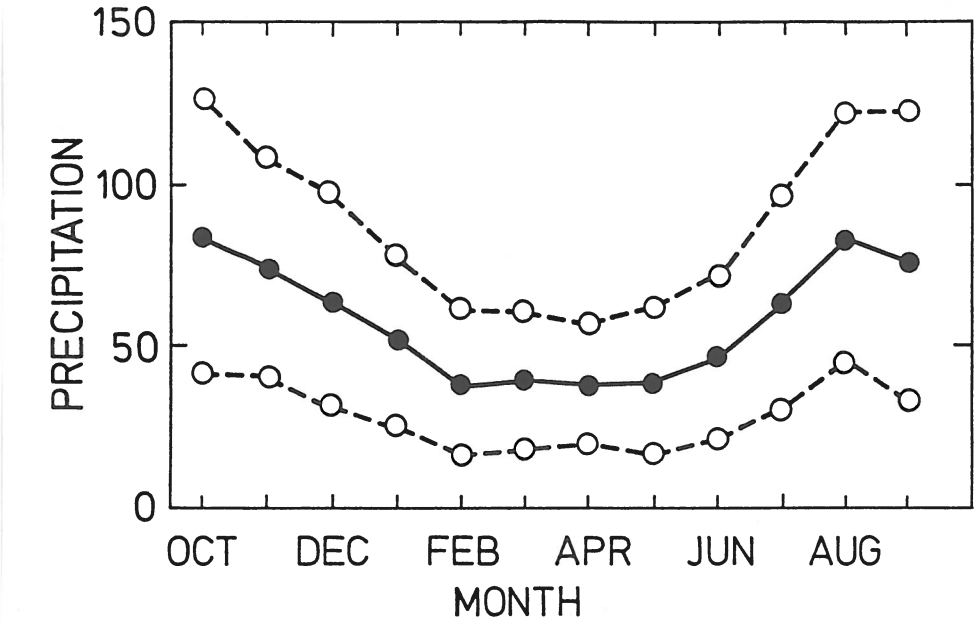

Fig. 4.4. Annual variation of monthly precipitation on Fanø with standard deviations (Peterson, 1983).

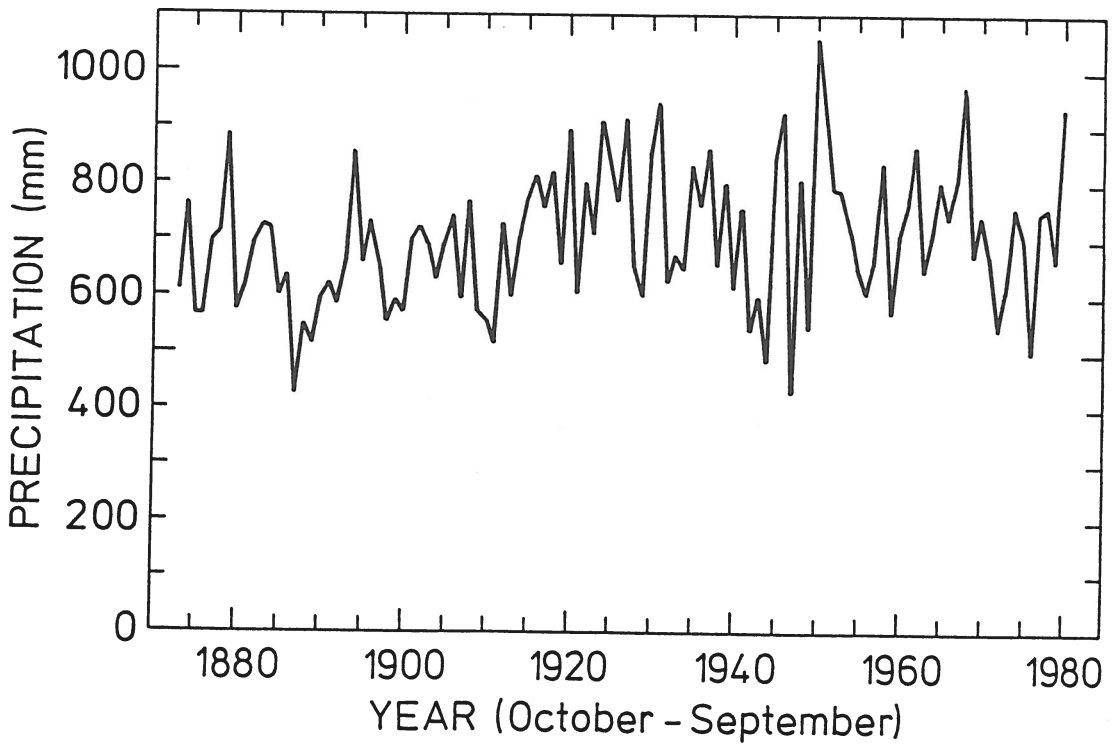

Fig. 4.5. Annual precipitation on Fanø as function of the year (Peterson, 1983).

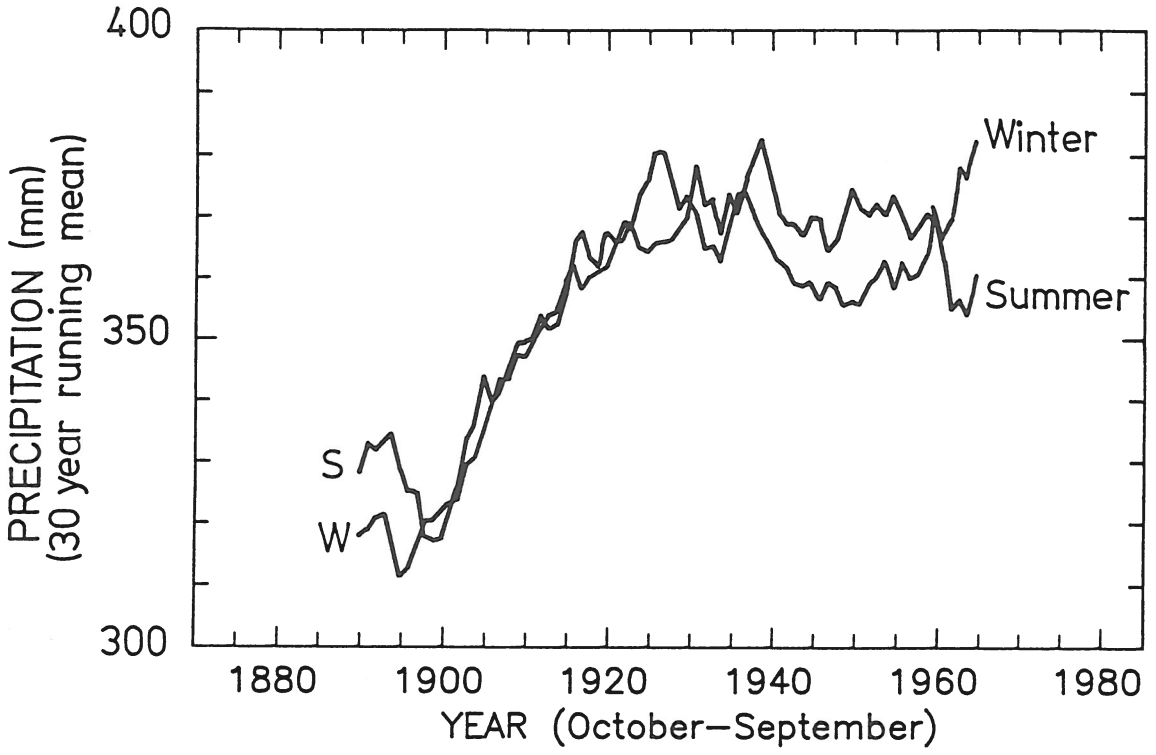

Fig. 4.6. Thirty-year running means of the data of precipitation for the six-month summer and winter periods (Peterson, 1983).

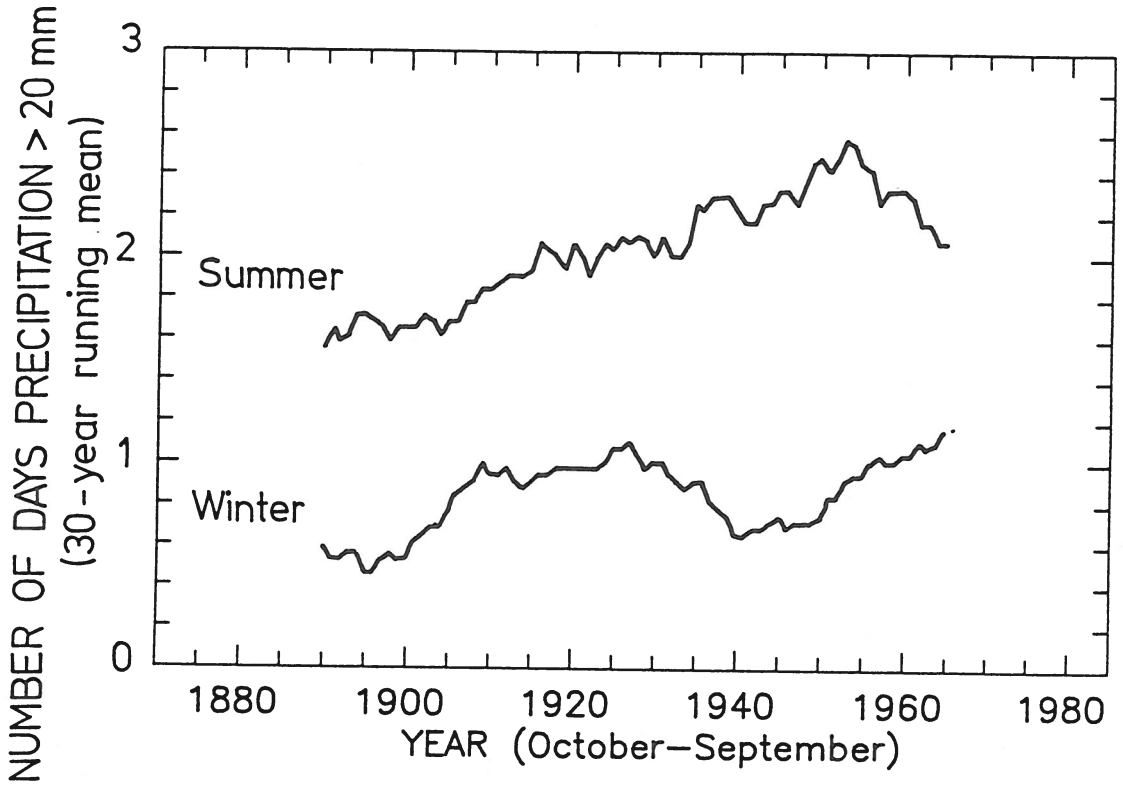

Fig. 4.7. Thirty-year running mean of the number of days with daily precipitation larger than 20 mm in the six-month summer and winter periods (Peterson, 1983).

4.3 Pressure data on Fanø

To a large extent pressure can be considered as the basic meteorological variable, since pressure gradients are the main driving force for atmospheric flows. From a more practical point of view we note that high pressure situations are associated with low winds, large diurnal temperature variation and, if they last long enough, air pollution episodes. Low pressure, on the other hand, is associated with passing cyclones, windiness and precipitation. Therefore, periods with much pressure variability is often characterized to be more windy than periods with low pressure variability.

Figure 4.8 shows the variation of the 5-year mean pressure together with the corresponding standard deviations, and it is remarkedly how the general decrease in pressure standard deviation is reflected through the period in the general decrease of windiness depicted in Figs. 3.7 and 3.11. A perfect correlation cannot be expected, since it is the pressure gradients that drive the flow, not pressure variations at a fixed point. Also, since the standard deviations shown are around 5-year mean values they will include more variability than just the synoptic changes of weather. Corresponding to the standard deviations, we show in Fig. 4.9 the standard deviations of selected fractile values also determined for consecutive 5-year periods. Due to the necessarily larger ordinate here than in Fig. 4.8 the variation is not so clear in Fig. 4.9. However, a closer inspection reveals that the difference between the 95 per cent and 5 per cent fractile has decreased during the duration of series.

The decreasing pressure variability depicted in Figs. 4.8 and 4.9 is illuminated further in Fig. 4.10, which shows the 30-year running mean of the number of cyclones passing Fanø (Peterson, 1983) . This is determined as the number of events in which the presssured dipped below 990 mb before raising again to more than 1000 mb. Here also the downward trend is obvious.

The 30-year running means of pressure at the three times of observation are shown in Fig. 4.11. Here a diurnal variation comes through very clearly. The variation is shown by Jensen (1984) to be associated with atmospheric tidal motion induced by the solar heating of the upper atmosphere. In Fig. 4.12 the measurements on Fanø are compared with the amplitude and phase of the dominant (twice a day) tidal wave mode at the geographical position of

Fanø as given by Chapman and Lindzen (1970). The agreement is excellent and supports the quality of data.

In Fig. 4.12 the yearly variation of the monthly mean pressure is shown as averaged over 30 years around four different years spaced along the duration of the series. The figure shows distinct differences between the periods considered but also the general behaviour of Danish weather comes through clearly with tendencies of high pressure weather in a winter period (January and February), an early summer period (May, June), and a late summer/early fall period concentrated around September. The absence of a yearly period is obvious also in the power spectrum in Fig. 4.13, which shows a broad maximum around 15 days and only a very small peak at the yearly period.

To a further study of the behaviour of the pressure signal we computed the joint frequency distribution, $F(p,\dot{p})$ of the daily mean pressure p and its derivative, $\dot{p}$ (the latter being mesured in mb per day) for the period 1873-1978. The marginal distributions $P(p)$ and $Q(\dot{p})$ are shown in Figs. 4.15 and 4.16, respectively, while the contour lines of the joint distribution are depicted in Fig. 4.17.

The pressure distribution $P(p)$ is slightly skew and is seen to be quite well described by a three-parameter Weibull distribution with the parameter values indicated in the figure. The three-parameter Weibul distribution is defined by

$$P(p) = \frac{1}{\Gamma(1/k)} \frac{k}{p_0} \left(\frac{p}{p_0}\right)^{l-1} \exp\left(-\left(\frac{p}{p_0}\right)^{k}\right) \quad , \tag{20}$$

and comparison with Eq. (4) reveals how the additional parameter ℓ is introduced. In an ordinary two-parameter Weibull distribution $\ell = k$.

The pressure change distribution $Q(\dot{p})$ is seen to be rather symmetric with a mean value of $\dot{p} \simeq 0$. It is seen that $Q(\dot{p})$ is quite well described by a normal distribution. Further the contours of the joint distribution $F(p,\dot{p})$ show the $\dot{p}$-marginal distribution to be fairly independent of p. Based on this we assume p and $\dot{p}$ to be statistically independent variables. Therefore, the joint distribution $F(p,\dot{p})$ is simply related to the two marginal distributions

$P(p)$ and $Q(\dot{p})$ as

$$F(p,\dot{p}) = P(p) \cdot Q(\dot{p}) \quad , \tag{21}$$

and it becomes easy to give an explicit expression for the average number of time $N_+(T,p')$. The pressure exceeds a certain positive deviation, $p' = p - < p >$, during time T (Panofsky and Dutton, 1984).

$$N_+(T,p') = T\frac{\sigma(\dot{p})}{\sqrt{2\pi}}P(< p > +p') for \text{ for } p' > 0 \tag{22}$$

with a corresponding expression for the number of times the pressure get below a pressure $p =< p > -p'$.

$$N_-(T,p') = T\frac{\sigma(\dot{p})}{\sqrt{2\pi}}P(< p > -p') \text{ for } p' > 0 \quad . \tag{23}$$

From Eq. (22) and (23) we can find that the average time p spends above $< p > +p'$ or below $< p > -p'$

$$\begin{aligned} T_+(T,p') &= T \int_{<p>+p'}^{\infty} P(p)dp \\ T_-(T,p') &= T \int_{0}^{<p>-p'} P(p)dp \quad , \end{aligned} \tag{24}$$

where $P(p)$ is given by Eq. (20) and shown in Fig. 4.15.

Thus, the average durations t_+ and t_- of positive and negative pressure excursions from the mean become

$$t_+(p') = T_+(T,p')/N_+(T,p')$$

$$t_-(p') = T_-(T,p')/N_-(T,p') \quad . \tag{25}$$

Note that t_+ and t_- are independent of T.

In Figs. 4.18 and 4.19 we compiled these parameters for the pressure signal at Fanø. Figure 4.18 shows the average number of high and low pressure events as functions of the pressure deviation from the mean pressure. Correspondingly, Fig. 4.19 shows the average duration (in days) for high and low pressure excursions of given magnitudes.

From the figures it appears that moderate high-pressure events occur more frequently than low-pressure events, while the situation reverses for extreme pressure excursions ($p' > 20$ mb). For almost all excursion of the daily mean pressure, low-pressure events last longer than high-pressure events.

As more specific examples we see that a high-pressure episode with daily mean pressure larger than 1025 mb on the average lasts 3 days and occurs 0,045 times per day or 16 times per year. A corrresponding low-pressure example with a daily mean pressure less than 990 mb on the average lasts 3.5 days and occurs 0.012 times per day or 4.4 times per year.

It is interesting to compare these findings for the low-pressure excursion with the findings of Peterson (1983), who counted that on the average the pressure dips below 990 mb with a return to 1000 mb 7-8 times a year, see Fig. 4.10. The difference between the 4.4 times based on the statistical model description and 7-8 times for the simple counting procedure is found because in the model computation we demand that the daily mean pressure shall be less than 990 mb, while in the counts of Fig. 4.10 we only demand that one of the daily observations should dip below 990 mb.

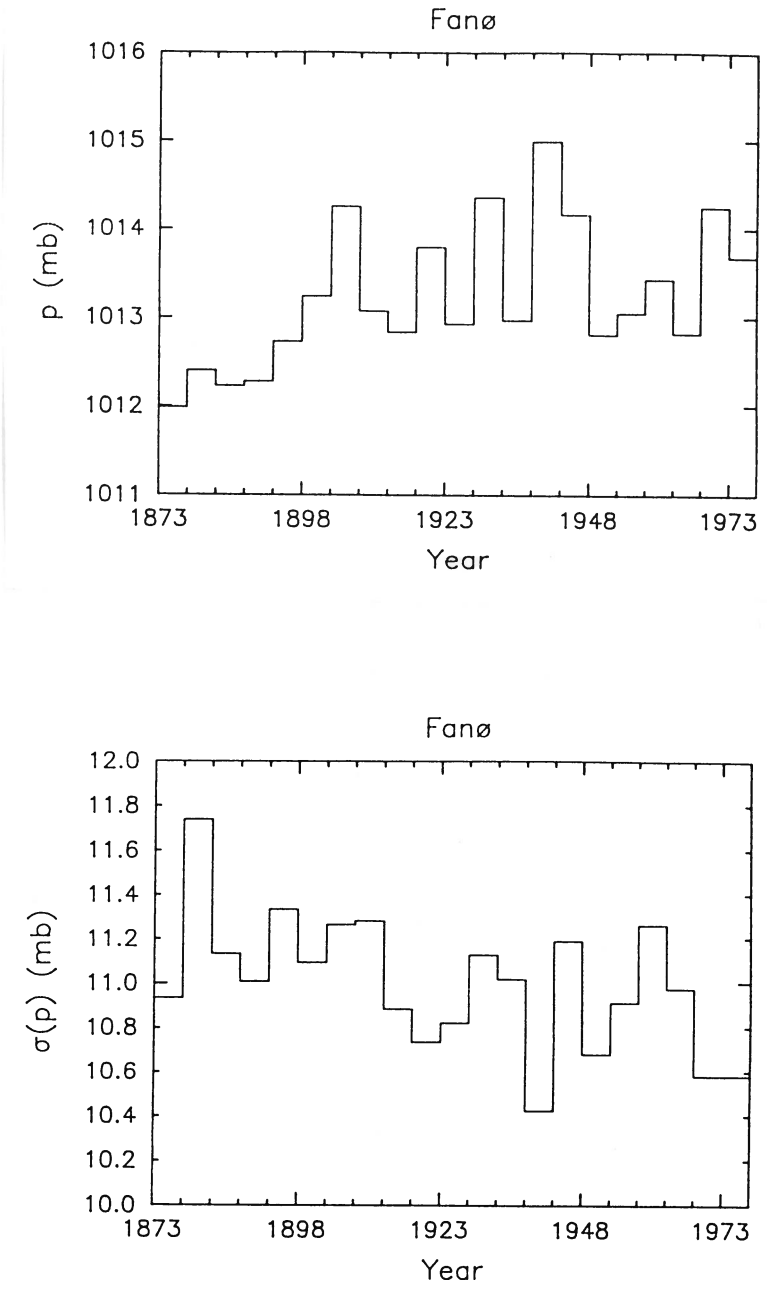

Fig. 4.8. Five-year mean values of pressure on Fanø with associated standard deviations.

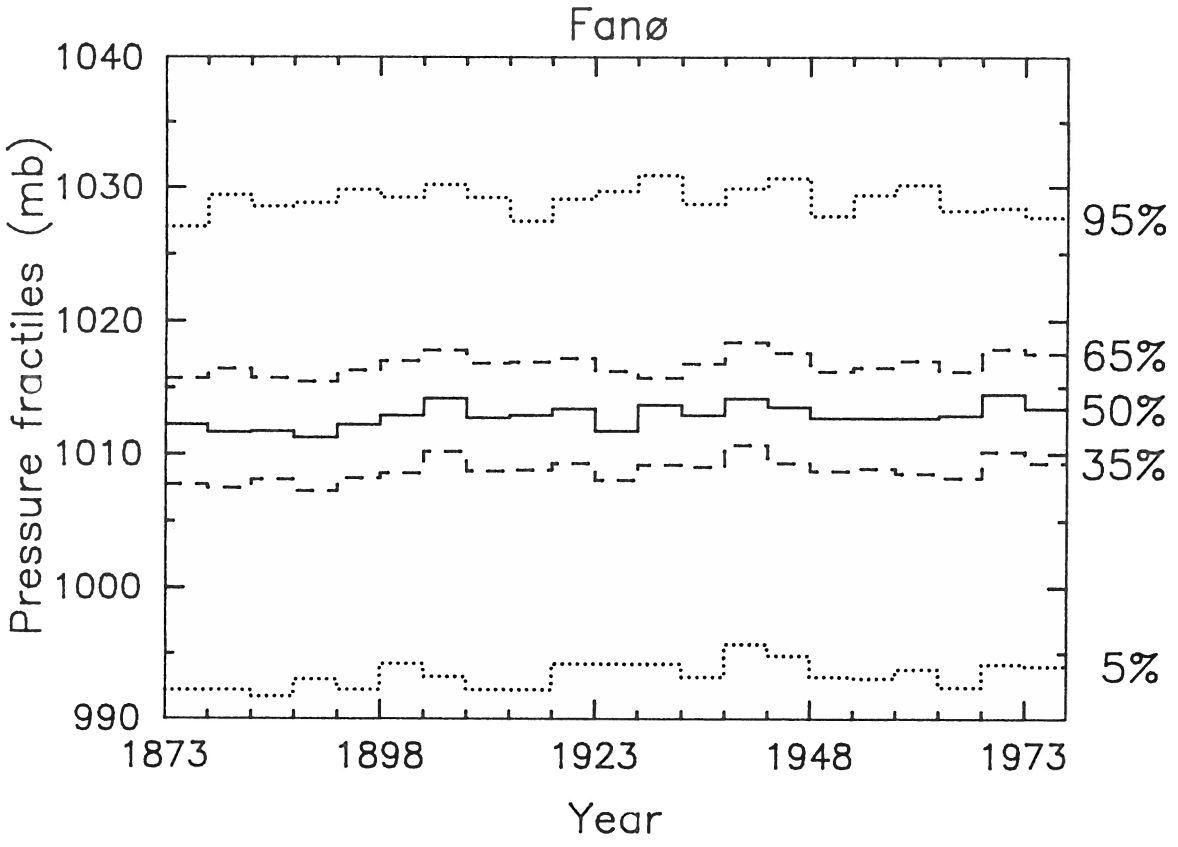

Fig. 4.9. Five-year values of fractiles of pressure on Fanø.

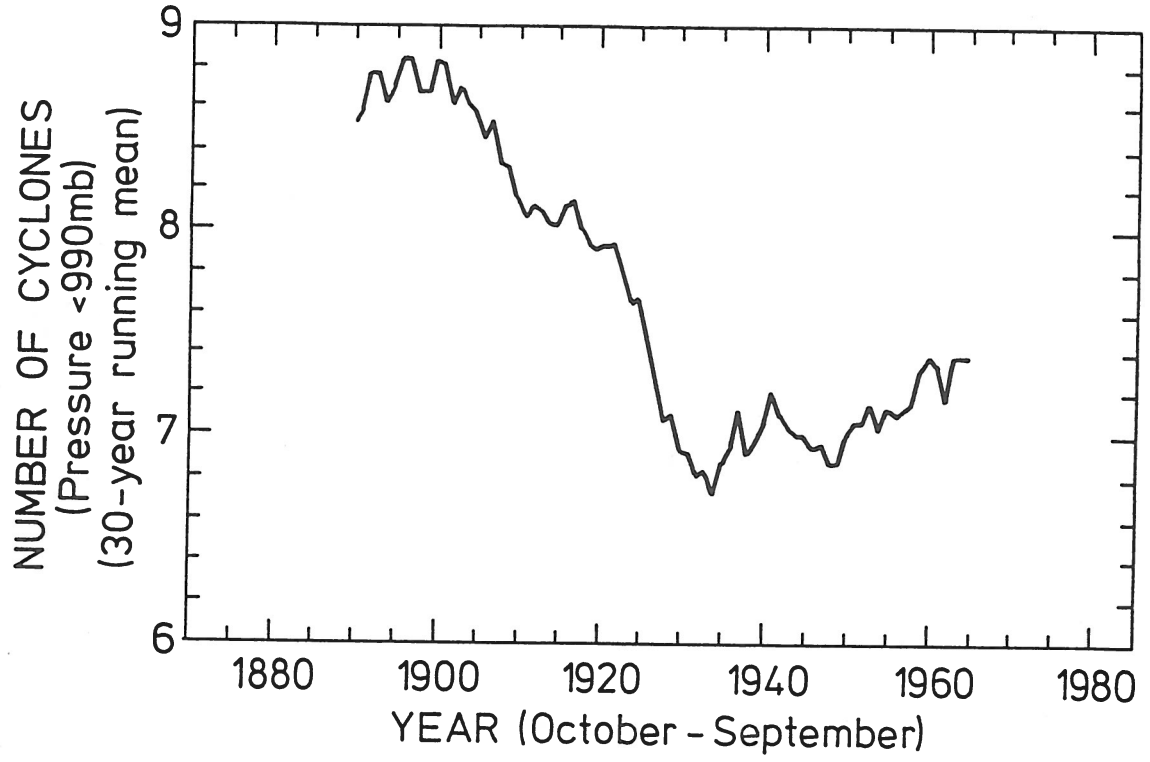

Fig. 4.10. Thirty-year running mean of the annual number of cyclones (pressure < 990 mb) passing Fanø (Peterson, 1983).

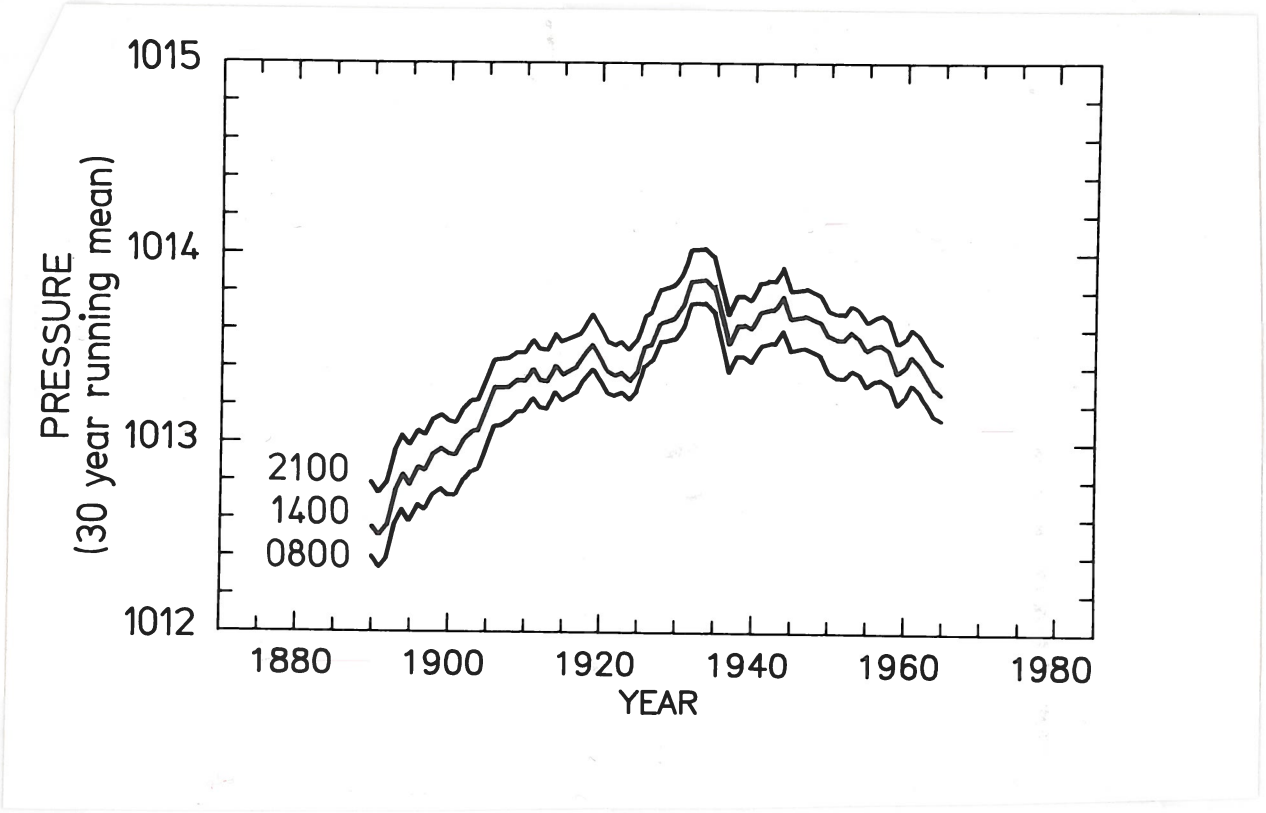

Fig. 4.11. Thirty-year running average of the pressure on Fanø at the three times of observation (Peterson, 1983).

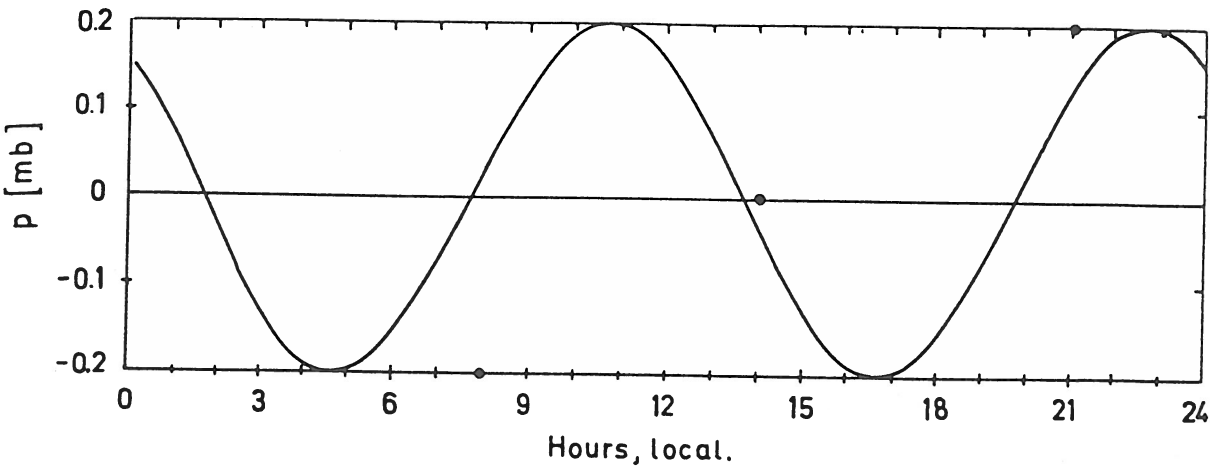

Fig. 4.12. Comparison between the dominant tidal wave component at the lcoation of Fanø and the measurements (Jensen, 1984). The measurements are indicated by the three points.

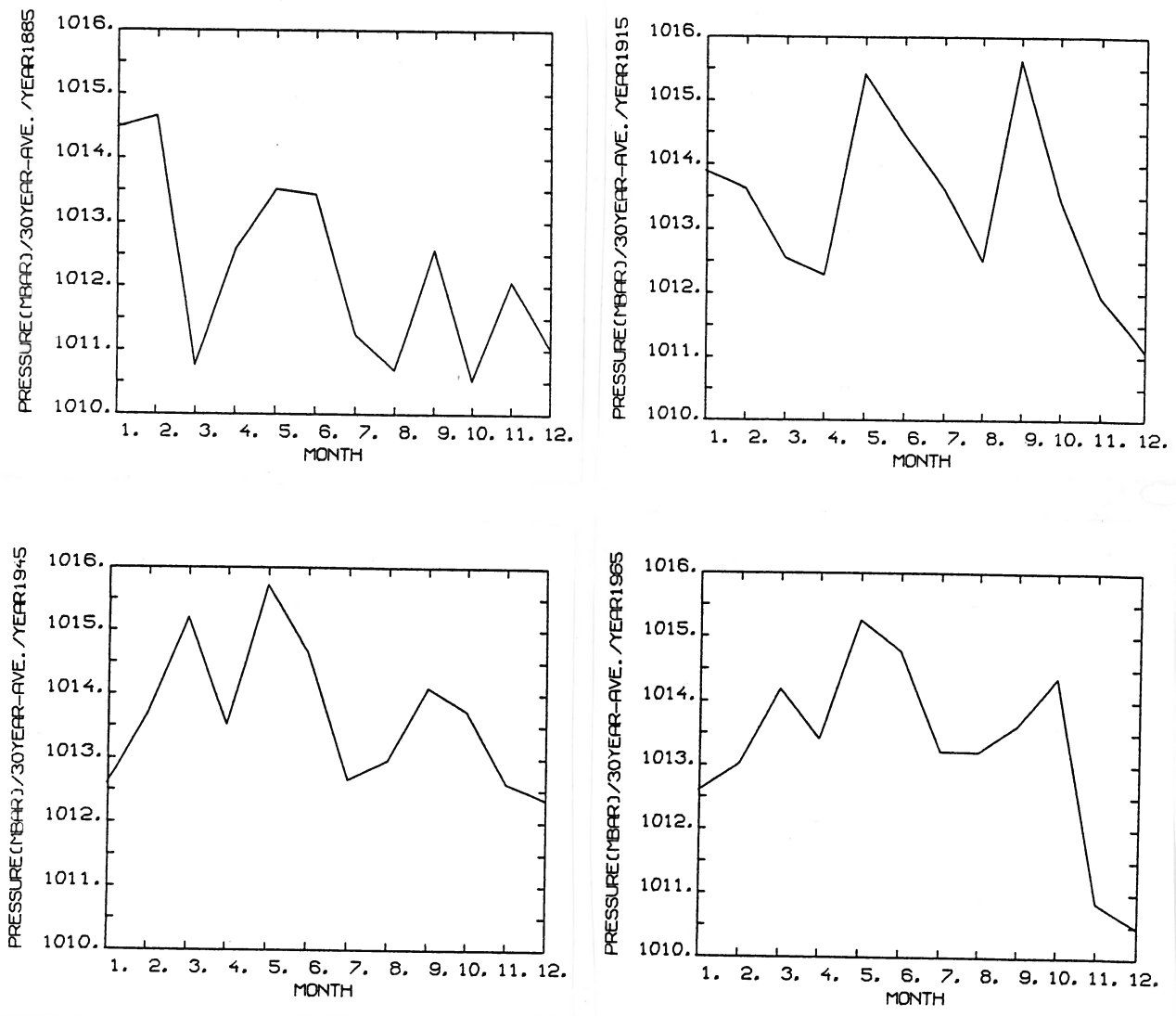

Fig. 4.13. The yearly variation of pressure averaged over 30 years around four different years, 1885, 1915, 1945 and 1965.

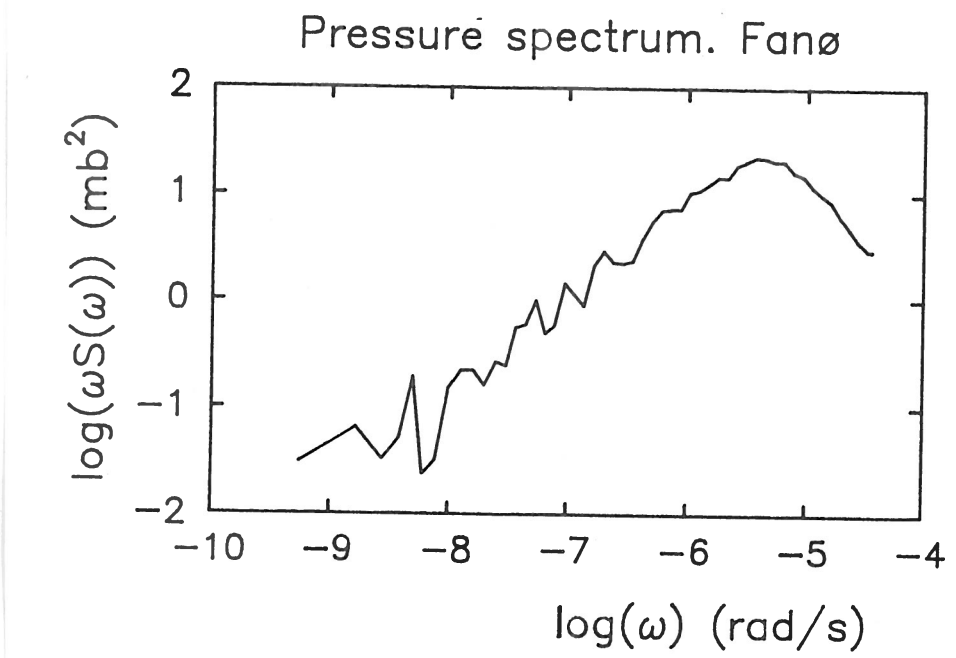

Fig. 4.14. Power spectrum of the pressure signal on Fanø. Note the almost total absence of a yearly period (2 10^{-7} rad/sec).

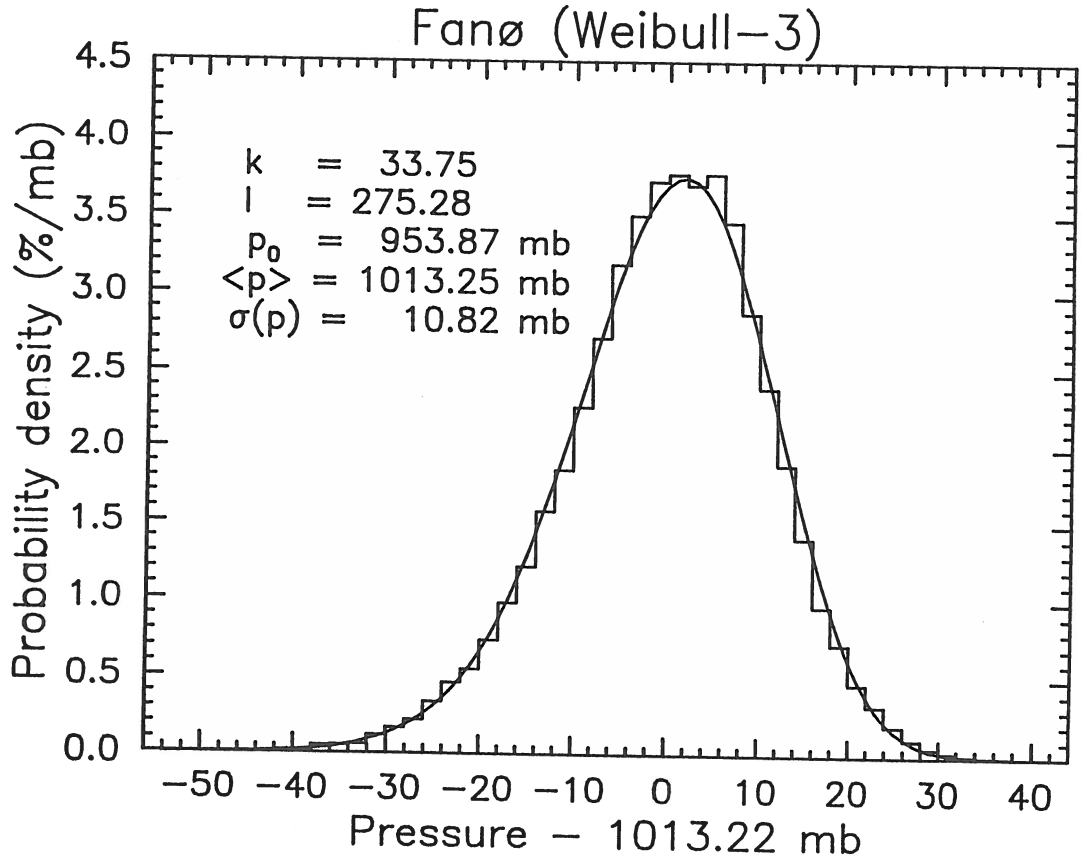

Fig. 4.15. Frequency distribution of the pressure on Fanø for the period 1873-1978. The curve is a three-parameter Weibull distribution with the parameter values indicated, compare Eq. (20).

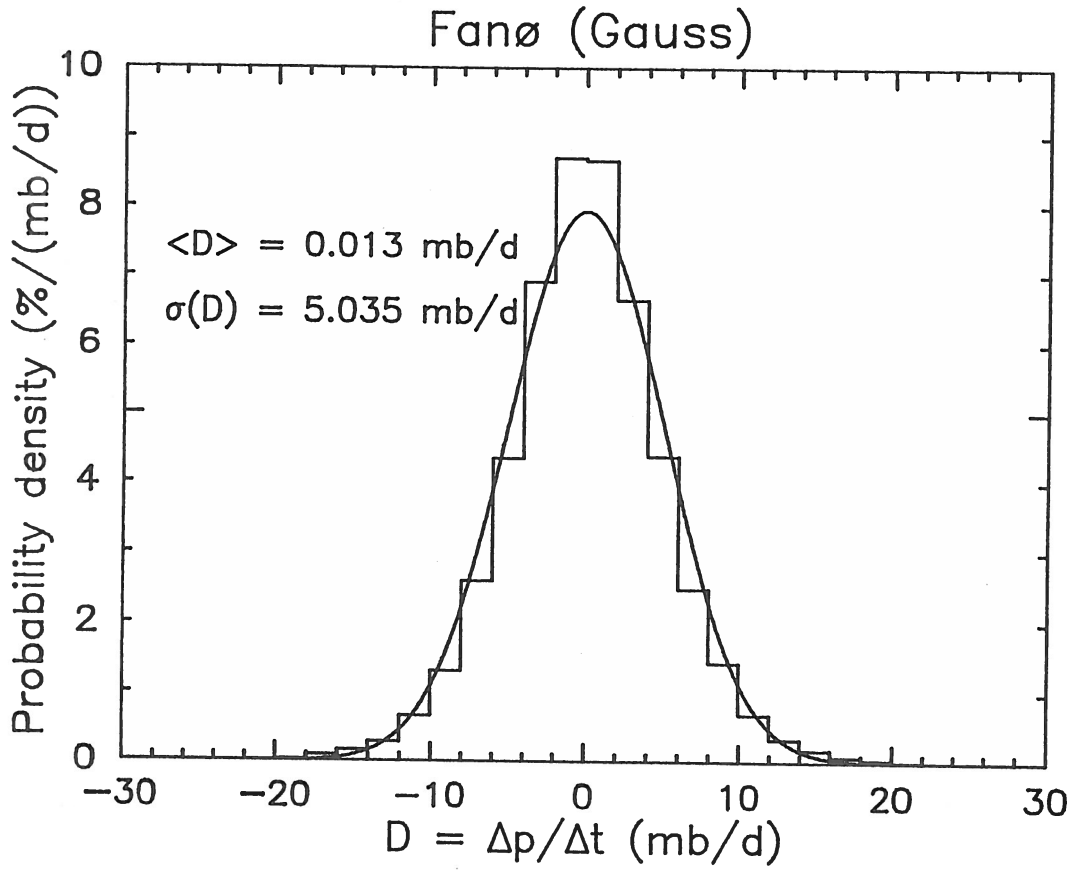

Fig. 4.16. Frequency distribution of the daily pressure change, $Q(\dot{p})$ on Fanø for the period 1873-1978. The curve is a Gaussian with the parameters indicated.

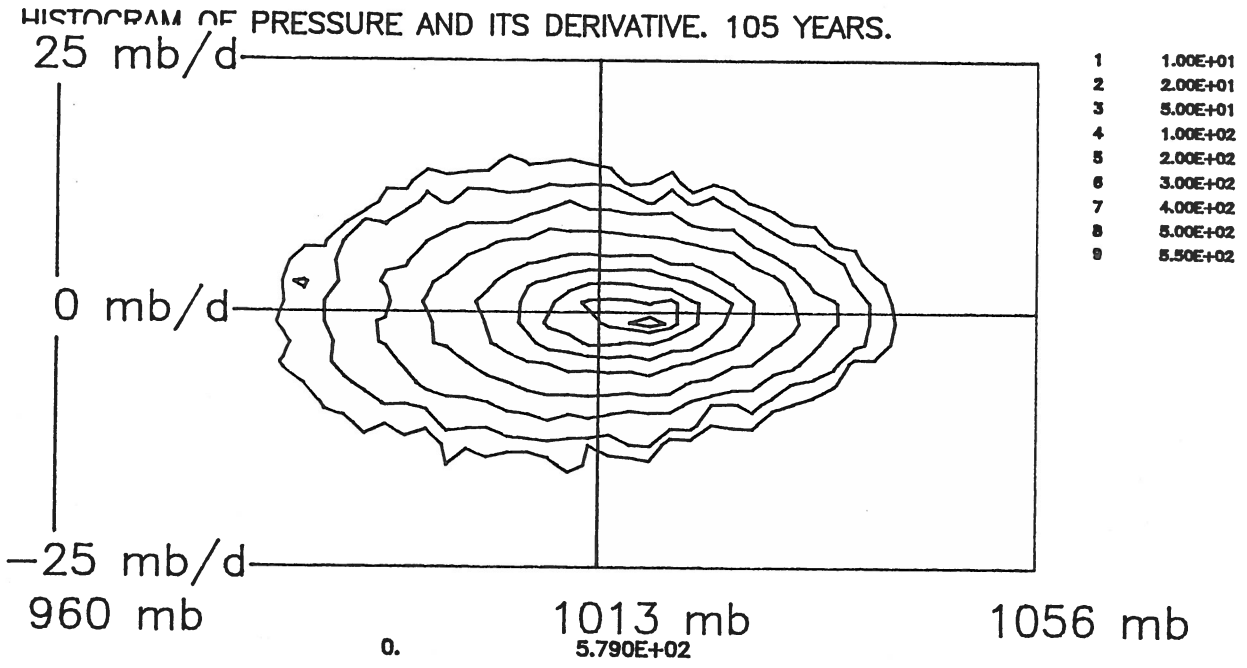

Fig. 4.17. Contour lines for the joint distributions of $(p, \dot{p})$. The abscissa shows p, while the ordinate is $\dot{p}$.

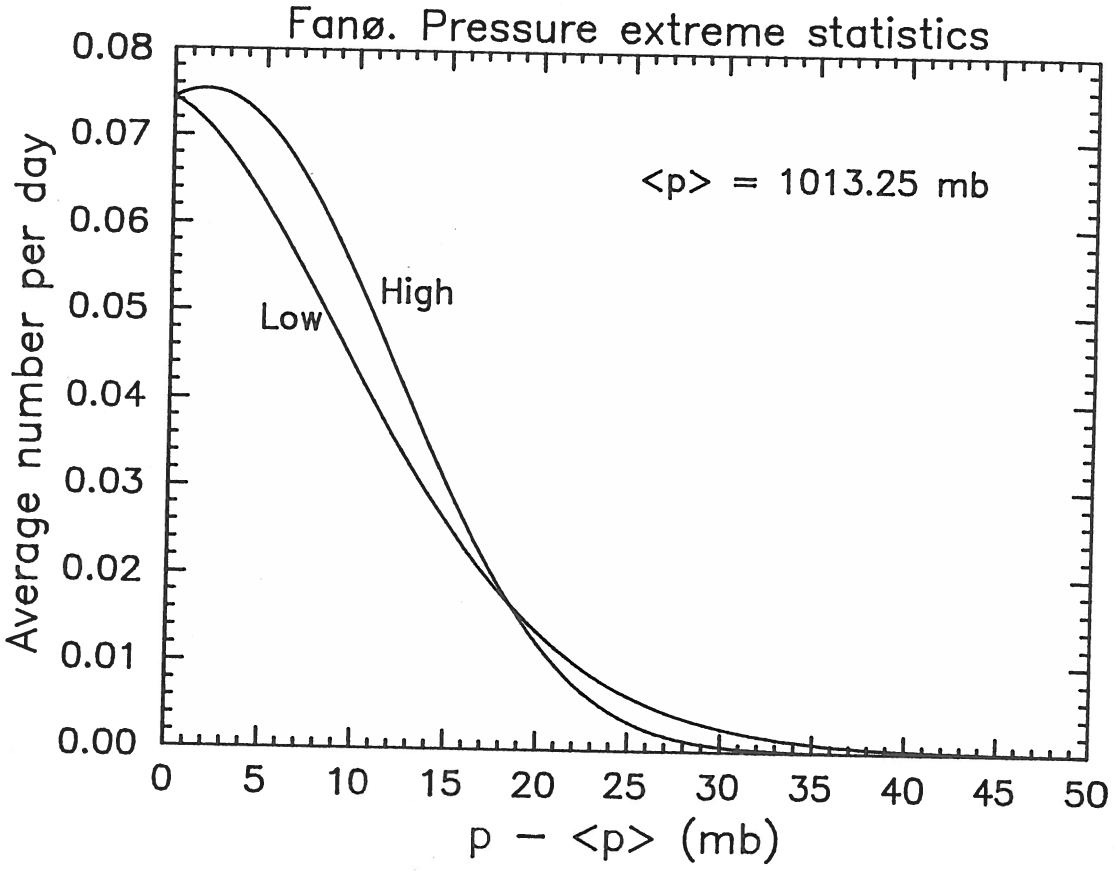

Fig. 4.18. Number of events per day where the deviations from the mean pressure exceed a given value for both high and low pressure events, compare Eqs. (22) and (23).

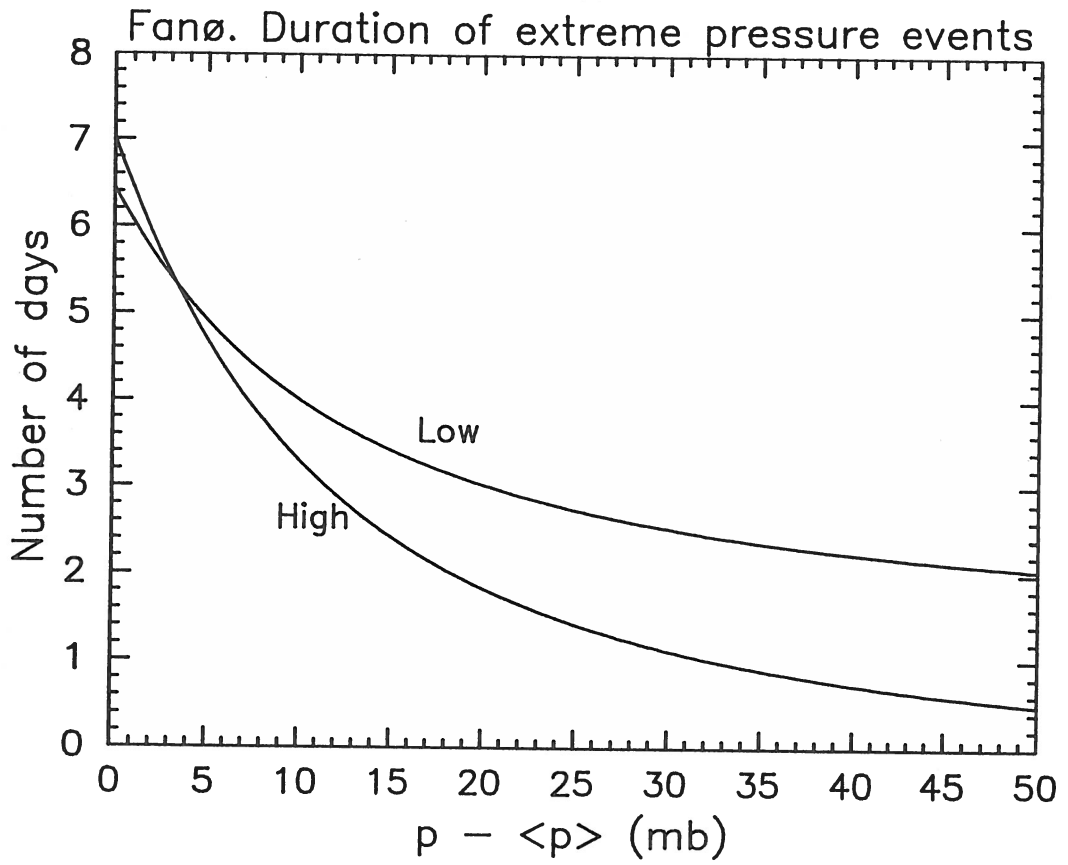

Fig. 4.19. Average duration of high and low pressure events where the daily mean pressure, p, deviates from the mean $< p >$ as a function of the pressure deviation.

5 Conclusions and discussion

From the study a shift emerges in climate initiated before start of the series (1872), culminating in the 1940'ies and followed by a somewhat uncertain steadiness till today. The shift can be described by an increasing tendency to high-pressure weather, increasing temperature, increasing precipitation with increasing shower frequency, and a decreasing windiness with a corresponding decrease in pressure varibility. These tendencies have been reported elsewhere for a large part of Northwestern Europe (Lamb, 1969) so within this theme the results of the present study is merely to support and quantify the general tendencies.

The above observations can be qualified with respect to two aspects. For the mean temperatures and the solar radiation, quite large variabilty is present between the two stations used in this study, indicating that climate has varied more across the country in periods than we are used to thinking, at least for these two parameters. For the wind energy potential we note that in spite of the decreasing mean wind, the wind energy potential shows little trend, a factor that might be owing to a change in the frequency distribution of the wind in a way that compensates to a certain extent for the changing mean wind.

As a standard the study has employed 5-year mean values of the parameter of interest, but used also other averaging times when prudent. We made little effort to make refined tests for trends and accurate estimates of variability, the philosophy being that only tendencies coming out clearly were worth a consideration and only as an order of magnitude estimates. This is so because the purpose of the study partly was to indicate the magnitude of changes to be expected in the near future, i.e. within the next 100 years.

With these limitations we have compiled in Table 5 a summary of our findings concerning trends and variability of the different parameters considered.

Table 5.1. Trends and variability for the 5-year averages of the different parameters considered. The trends are indicated in the units considered most appropriate for each parameter, and is always understood as change from the start of the series till today. The varibility is a typical variability of the individual 5-year values around the line of trend.

Parameter	No. of series	Trend	Variability	Section
Temperature	2	1.5°C	±1°C	3.1
Degree days	2	- 10%	±10%	3.1
Solar radiation	2	0%	±10%	3.2
Wind speed	2	-2 m/s	± 1 m/s	3.3
Wind energy	1	0%	±30%	3.4
Freq. stab. class	2	0%	±5%	3.4
Mean conc. $\bar{\chi}$	1	0%	±50%	3.4
$\chi_p(p{=}1\%)$	1	0%	±55%	3.4
Precipitation	1	+15%	-	4.2
Pressure, p	1	+ 2 mb	± 1 mb	4.3
$\sigma(p)$	1	-5%	±5%	4.3

A part of the discussion must necessarily consider the validity of our results in the light of both the data and models applied.

From a model point of view the description of heating degree days and wind energy is most reliable in the sense that the models used are well tested, and there was no need for introducing additional assumptions to adapt the models to available data. The description of the air pollution concentration is most uncertain in that our results depend on a number of strongly simplified assumptions that is undoubtedly not true for for the station (Hesselø) at which we applied the full model description but where we have to fall back on arguments concerning the general validity of our approach. With respect to reliability, our description of the available solar energy is in between degree days and wind energy on one side and air pollution of the other. Here we used a simplistic, but generally accepted formula to relate the incoming radiation to the cloud cover index available from the two data series applied. The accuracy of the data is the other side of the realibility issue. We controlled the transcription of observations to computer tape by checking for "outliers" by various statistical tests that

could be applied. Since the velocity observations at Hesselø came out to be the only really reliable series of wind speed that has come out of this study, it was furthermore controlled by comparing our data series to another series of monthly wind speed statistics independently compiled from the same observations. The other check applied is the consistency one. Basically we have checked to what extent the different signals behave in an expected way. We also checked to what extent observed differences between the two stations involved are in accordance with our general knowledge about the differences between the two stations – physically, meteorologically and climatologically. Throughout this report we have repeatedly referred to these checks and control considerations when discussing the individual parameters. Here we shall limit ourselves to state that the result seems to show a high degree of consistency in the variation of parameters studied.

In conclusion of this discussion we should like to mention, however, two features of the data that must so far be unsolved.

One concerns the somewhat small k-values of the wind speed distributions. This is a common experience for observed wind speeds rather than measured ones, as discussed in section 3.3. Although it undoubtedly influences our estimates of U^3, we believe that due to the cut-off character of the power curve in Fig. 3.12, its influence on the wind energy potential in Fig. 3.13 is considerably less. The other feature is the periodically large variation between Hesselø and Fanø with respect to mean temperature and solar radiation (cloud cover), compare Figs. 3.2 and 3.5. The variations indicated between the two sites certainly are conceivable from a climatological point of view. No obvious reasons are found in the records or data indicating it to be a measuring problem, though especially the temperature deviations seem large. We will refer these result to further studies while we note for now that our conclusions presented in Table 5.1 are insensitive to future corrections of these data if such indeed will be made.

6 Acknowledgements

It appears from the list of publications that many people have been involved in work with the data used in this project. Apart from the authors of the publications we wish to acknowledge the important contributions by Morten Frederiksen and Lennart Christensen in organizing the Risø and Hesselø data, respectively. Also support and assistance by A.W. Hansen, L. Christensen, N.O. Jensen, E.L. Petersen and I. Troen is gratefully acknowledged.

7 References

Publications within the contract

Jensen, N.O. (1984). Tideluft (Tides in the air). *Vejret*, **6**, 30-33.

Kristensen, L., Larsen, S.E. and Frydendahl, K. (1988). Klimatisk variation af energirelevante parametre i Danmark (climatic variation of parameters relevant to energy in Denmark). To appear in *Vejret*.

Larsen, S.E. and Jensen, N.O. (1983). Summary and interpretation of some Danish climate statistics. Risø Report No. R-399.

Larsen, S.E. (1985). Impact of climatic variability on wind and solar energy production, on heating consumption, and on dispersion of pollutants. In: Report on First R&D Programme in the Field of Climatology 1981-85. Eds. R. Fantechi and A. Ghazi, CEC, Luxembourg, 229-235.

Nielsen, N.W. and Hansen, A.W. (1986). Vejrets rytme på Fanø (the synoptic rythm at Fanø). *Vejret*, **8**, 24-26.

Peterson, E.W. (1983). A study of the weather record from Fanø (1872-1980) including an analysis of climate variation. Risø Report No. R-483.

Peterson, E.W. and Larsen, S.E. (1983). Klimatiske ændringer over de sidste hundrede år ved Fanø (climatic changes during the last one hundred years at Fanø). *Vejret*, **5**, 18-20.

Peterson, E.W. and Larsen, S.E. (1984a). Climatic variation on Northern Europe during the past century. Evidence from a Danish record. In: Climatic changes from a yearly to millenial basis. Eds. N.A. Mörner and W. Karlén, E. Reidel Publishing Co., 371-379.

Peterson, E.W. and Larsen, S.E. (1984b). Analyse af vindobservationer fra Fanø i perioden 1872-1980 (Analysis of wind observations from Fanø in the period 1872-1980). *Vejret*, **2**, 12-17.

Other publications referred in the text

Blackadar, A.K. (1984). A computer almanac, Weatherwise, October, 257.

Brown, N., Olesen, H.R., Prahm, L. and Reiter, A. (1983). Kvalitetskrontrol af Fanø klimadata. Miljøstyrelsens Luftforureningslaboratorium, Risø, Report No. MST-Luft-A75.

Chapman, S. and Lindzen, R.S. (1970). Atmospheric tides (Reidel Publishing Co.).

Holtslag, A.A.M. and Van Ulden, A.P. (1983). A simple scheme for daytime estimates of the surface fluxes from routine weather data. *J. Clim. Appl. Meteor.*, **22**, 517-529.

Klug, W. (1969). Ein Verfahren zur Bestimmung der Ausbretungsbedingungen aus Synoptischen Beobachtungen. Staub-Reinhalt. *Luft*, **29**, 143-147.

Lamb, H.H. (1969). Climatic Fluctuations. World Survey, Vol. 2. Ed. H. Flohn, Elsevier, Amsterdam.

Larsen, R.I. (1969). A new mathematical model of air pollutant concentration, averaging time and frequency. *J. APCA*, **19**, 24-30.

Larsen, R.I. (1973). An air quality data analysis system for interrelating effects, standards and needed source productions. *J. APCA*, **23**, 933-940.

Larsen, S.E. and Petersen, E.L. (1974). Statistical description of air-pollution concentration, averaging time and frequency. In: Proceedings of Symposium on Atmospheric Diffusion and Air Pollution, Santa Barbara, California, AMS, Boston, MA, 163-167.

Panofsky, H.A. and Dutton, J.A. (1984). Atmospehric Turbulence. (John Wiley & Sons).

Petersen, E.L., Troen, I., Frandsen, S and Hedegaard, K. (1980). The Danish Wind Atlas. A rational method of wind energy siting. Risø Report No. 428.

Petersen, E.L. and Troen, I. (1986). The European Wind Atlas. In: Proceedings of European Wind Energy Association Conference and Exhibition, Rome, October 86. Eds. W. Palz and E. Sesto, Published by A. Raguzzi, Rome, Vol. I, 93-98.

Troen, I., Mortensen, N.G. and Petersen, E.L. (1987). WA^{S}P , Wind Atlas Analysis and Application Programme. Dept. of Meteorology and Wind Energy, Risø National Laboratory, Roskilde, Denmark.

Turner D.B. (1964). A diffusion model for an urban area. *J. Appl. Meteor.*, **3**, 83-91.